STRUCTURAL HEALTH MONITORING FOR BRIDGES USING ADVANCED DATA ANALYSIS FOR PROCESS NON-LINEARITY AND NON-STATIONARITY

By

ERMIAS BIRU

Bachelor of Science in Industrial Engineering
Bahir Dar University
Bahir Dar, Ethiopia
2004

Submitted to the Faculty of the
Graduate College of the
Oklahoma State University
in partial fulfillment of
the requirements for
the Degree of
MASTER OF SCIENCE
December, 2010

STRUCTURAL HEALTH MONITORING FOR BRIDGES USING ADVANCED DATA ANALYSIS FOR PROCESS NON-LINEARITY AND NON-STATIONARITY

Thesis Approved:

Dr. Zhenyu (James) Kong

Thesis Adviser

Dr. Tieming Liu

Dr. Tyler Ley

Dr. Mark E. Payton

Dean of the Graduate College

ACKNOWLEDGMENTS

I would like to express my deepest appreciation to my advisor, Dr. Zhenyu (James) Kong, for his continuous support, patience and excellent guidance throughout my study. I learned many important lessons from him and he is always there to listen, advise and motivate me.

I would like to thank Dr. Tieming Liu and Dr. Tyler Ley for serving on my thesis committee as well as for their valuable input throughout my study and during my thesis defense. I am grateful to Dr. Ley for his support in providing the data used for analysis.

I am also grateful for the support and guidance that I had from my senior and doctoral students Mr. Asil Oztekin and Mr. Omer Beyca. I am also thankful to Mr. Mahmoud Z. Mistarihi for his suggestion and help in organizing the document.

This thesis would not have been possible without the help of my parents Mrs. Aberu Abtew and Mr. Belay Biru who encouraged me from the initial to the final level of my study. I am also grateful to the support I had from my sisters and brothers.

Finally, I offer my regards to Mr. Getachew Tsegay, Mr. Kumlachew Woldesenbet, and others who supported me in any respect during my study.

TABLE OF CONTENTS

Chapter Page

LIST OF TABLES

Table Page

LIST OF FIGURES

Figure Page

Figure Page

CHAPTER I

INTRODUCTION

1.1 Research Motivation

There are more than 600,000 highway bridges in the united states ASCE (2009). Guidelines by the AASHTO (2007) suggest that the expected service life of a bridge to be a minimum of 75 years. The majority of bridges currently in use were built after 1945. However, significant environmental damage requiring repair typically occurs before the average bridge reaches mid-life. In 2005, the ASCE estimated that it would take $188 billion over the next 20 years to eliminate bridge deficiencies in the United States (ASCE, 2005). The cost of delaying these repairs is significant as delay leads to increases in road user costs, material, and construction costs.

It is possible that the condition or health of these bridges could be effectively monitored by using sensors. Using sensor information, more informed repair and maintenance decisions could be made. Furthermore, these sensors may be able to give the local state Departments of Transportations (DOTs) information about when a bridge is nearing the end of its usable life. While this could be a useful tool, it is not currently cost-effective to monitor the health of common structures due to the high cost of sensors,

installation of these sensors and, ultimately, the monitoring of the sensor system. However, it has been found to be cost-effective by several DOTs to use structural health monitoring (SHM) on major “lifeline” or critical structures. These structures are of such great importance to the public that they must remain open and be maintained to last as long as possible.

According to the FHWA and US DOT (2009) report there are more than 600,000 bridges in the United States and 11.8% of the bridges are structurally defective and 13.01% are functionally obsolete and more than $17 billion is needed to improve the current condition of bridges. Visual inspection is the primarily method used to evaluate the condition of these bridges. SHM can help the decision making process of classification of condition of bridges by assessing the internal condition of the bridge structures where it would be inaccessible or uneconomical by the visual inspection approach. The consequence of ineffective inspection of bridges can be very severe. The collapse of the I-35W Mississippi River Bridge on August 1, 2007 in Minneapolis caused a loss of13 lives and the replacement cost for the bridge was about $234 million. Other costs are incurred as a result of increased commute times, loss of business from lack of local access, and lost revenue from the blockage of a major river shipping channel. According to the (NTSB, 2007) report the bridge is collapsed due to design defects and excess load at the time of the collapse.

1.2 Problem Statement

Components that directly affect the performance of the bridge must be periodically inspected or monitored. Currently, visual inspection is the primary method

used to evaluate the condition of most highway bridges. Inspectors periodically visit each bridge to assess its condition. This type of inspection is highly dependent upon the individual inspectors' experiences. Even for experienced inspectors, it is difficult to detect corrosion and crack development inside of structural elements, and almost impossible to realize the resulting changes in deflections of the structure due to local changes in stiffness. Moreover visual inspection is labor intensive and costly.

1.3 Research Objectives

Due to the shortcomings of traditional inspection methods and advancement in sensor technology and wireless data transmission, researchers have turned their attention to SHM in recent years. SHM is generally a type of non-destructive inspection (NDI) which allows the examination or testing of an object or material without affecting the operational life or causing damage. The ultimate goal of the research in this thesis is application of data processing methodologies and statistical techniques for response data acquired from sensors for the purpose of SHM. The objectives of this research include:

(i) Time series modeling and spectral analysis of data gathered from a normal working state and damaged state to validate the proposed signal processing tools.

(ii) Application of statistical tools to support the proposed signal processing approaches to be able to decide when damage occurs to a structure.

(iii) Prediction or forecasting of damage indicator parameters based on past recorded values.

1.4 Research Methodology

Damage to a civil structure can be detected by processing or analyzing response data obtained from sensors installed on the structure such as a bridge. The premise behind these response data analysis methodologies is that when damage occurs to a structure, it induces changes in the structural properties which results in loss of stiffness or a change in energy dissipations of the structure. These changes in turn will alter the measured dynamic response of the structure.

To detect the incurred damage, time series modeling and spectral analysis approaches are utilized in this research. High volume data from a functional bridge is analyzed in a step by step approach from a time series perspective. Frequency domain approaches which include Fourier transform, wavelet analysis and Hilbert transform were also applied on a simulation data of a benchmark problem. Comparison of the effectiveness and sensitivity of the methodologies was also the subject of this research. The main feature extraction or damage indicator parameter approaches used in this study were frequency changes in the spectral analysis tools while time series and statistical analysis tools were applied to detect the changes in the amount of deformation developed on a supporting column of a bridge.

1.5 Thesis Organization

Background and a detailed review of recent development of SHM are discussed in chapter 2. Prior studies conducted on feature extraction and signal processing for the purpose of SHM are also revised in this chapter. In chapter 3 proposed methodologies of data processing approaches and case studies to show the applicability of the methods are

described in detail. Chapter 4 presents the application of the proposed methodologies for data obtained from a currently working bridge and a benchmark simulation. Presented in chapter 5 are the conclusion and summary of the research work together with the recommendations for future study in this area.

CHAPTER II

LITRETURE REVIEW

2.1 Introduction to Structural Health Monitoring

According to (Sohn *et al*., 2003) Structural Health Monitoring (SHM) can be defined as "the process of implementing a damage detection strategy for aerospace, civil and mechanical engineering infrastructure". In this context, damage is defined as changes in the geometric or material properties of the infrastructures, which negatively affect the normal working condition. For example, a crack that develops on a supporting column of a bridge invokes a change in the stiffness of the column; hence it can be considered as damage.

2.2 Phases of Structural Health Monitoring

SHM deals with the observation of structures, such as, bridges or buildings, over a period of time; by means of response measurement data acquired from sensors, feature extraction from the measurement system and the application of statistical tools to detect the presence of damage.

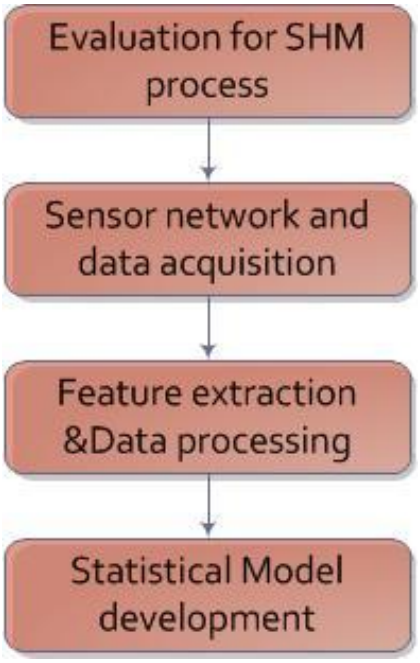

Fig.2.1 Basic steps in SHM system

2.2.1 Operational Evaluation

Operational evaluation is concerned with the scope of SHM system as a whole. It addresses the following issues:

(i) The need to conduct SHM for a particular structure under study.

(ii) Definition of damage to the structure.

(iii) The Operational and environmental condition under which the monitored structure exists or experiences.

Some of the major reasons in conducting SHM are economic and life style issues. For example, the collapse of the I-35 Mississippi Bridge resulted in death of 13 people and an economic loss amounting between 400 thousand to 1 million dollars.

Environmental and operational conditions should also be considered while implementing SHM. Doebling and Farrar (1997) state that the modal analysis of Alamosa Canyon Bridge in New Mexico depicts first mode frequency variation due to the temperature difference recorded within 24 hours. The implication here is that, changes in the surrounding conditions can produce a far more significant amount of variation on measured parameters compared with the actual damage progress experienced by the structure. Staszewki *et al*. (2000) discuss that ambient vibration and temperature could affect piezoelectric sensors negatively, which is mounted on composite plates. The delimitation in the composite plates was concealed by temperature variability. Rohrmann *et al*. (1999) found that a structure's material properties were altered as a result of change in temperature and this change resulted in a change in the reaction forces from the bridge supports. The authors also formulated a mathematical modal using regression to show the effect of temperature on the natural frequency.

$$\Delta f = a_0 T_0 + a_1 \Delta T \qquad 2.1$$

As the equation shows, there is a linear relationship between temperature change and natural frequency. According to the article by (Wong *et al*., 2001), the displacement response of a bridge is the combined effect of impacts, which arise from major sources of wind, temperature, highway, and railway. The authors further discussed the effect that temperature has on long suspension bridges. Temperature difference could cause damage to a bridge by forcing expansion and contraction of the bridge along the longitudinal direction. The effect of wind and rain-wind induced vibration on the performance of a bridge is discussed in the report by (Zuo *et al*., 2010).

2.2.2 Data Acquisition

The acquisition of data is one of the integral components of a modern SHM system. Issues such as how often to collect the data, the type, placement and number of sensors are also handled in this step. After the data has been produced, it is necessary to get this information from the data acquisition system and to the user to evaluate. Sampling and processing of signals, usually manipulated by a computer, to obtain the desired information is referred to as Data Acquisition (DAQ).

The components of data acquisition systems include appropriate sensors that convert any measurement parameters to electrical signals, which are acquired, displayed, analyzed and stored on a PC by interactive control software and hardware. A general understanding of this system and its components is essential in order to design an efficient and useful monitoring program. Generally, there are two common data acquisition systems, namely, the manual and computer based systems.

In a manual system, the operator visually reads the data from the read out units and records it manually. Since this system does not need bulky equipments, it is an economical and convenient way to collect data from a small number of sensors within a short period of time. However, for more general applications, a computer based acquisition system must be used. The components of this data acquisition system are signal conditioners, one or more data acquisition boards, and a computer.

2.2.2.1 Excitation Methods

Prior to obtaining the data, there should be some sort of excitation method applied on the structure of interest. Generally, the excitation methods that we use to vibrate or set a structure in to motion can be categorized in to forced excitation and ambient excitation.

Forced excitation: in this category, a number of different excitations methods are applied. Some of the most commonly used are: actuators, shakers and a variety of methods of measured impact. Sohn *et al*. (2000) used actuators and electromagnetic shakers in order to excite a bridge concrete column. The benefit of this method is that the input force used to excite the structure under study is large enough that it reduces the effect of noise disturbances, which could have a stronger signal to noise ratio. Other subsection of forced excitation is the local excitation. Local excitation is a type of forced excitation whereby input force is applied where there is the need to excite a subsection of a particular structure of interest. The local excitation has a benefit of surpassing the effect of environmental and operational conditions to which a structure is subjected.

Ambient excitation: occurs to a structure while the structure is working under normal operating conditions. One major difference between ambient excitation and forced excitation is that it is not easy to measure the amount of input force from this source of excitations; unlike the forced excitation types, other ambient excitation differences are persistent consistently (Sohn *et al*., 2003). For example, a bridge is consistently influenced by ambient excitation sources. The major sources of ambient excitations are traffic, wind, wave motion, and pedestrians. These sources of excitations are the preferred alternatives while implementing SHM systems, since it indicates the actual and real time excitation of a structure. However, these sources of ambient

excitations may not be applicable to all types of bridges. Pedestrian excitations which are generated while people are walking on a bridge may not be applicable to a Highway Bridge. At the same time, excitation from traffic is uncommon to a small bridge which is found farther away from cities.

Once the source of excitation is studied, the next step would be measurement of the output from the excitations. Sensors are used to capture or to record the output from the different types of excitations. The premise of vibration or excitation based SHM is when a change in mechanical properties occurs; these changes are depicted in the response output measured. Response measurements from sensors are kinematic parameters, which include strain, displacement, acceleration and velocity. In addition to these parameters, temperature, wind, humidity are also recorded to examine the surrounding conditions of the structure.

2.2.2.2 Sensor Applications in SHM

Real-time data for bridge condition monitoring can be provided by embedded sensors installed on the structure of interest. The type of sensors to be installed is dependent up on the accuracy needed, type of bridge under investigation and the measurement of interest. The most common types of sensors used in bridge health monitoring are strain sensors. Strain sensors are measuring elements that convert force, pressure, tension, etc., into strain readings (Zalt *et al*., 2007). Through connection of sensors networks by using a wired or wireless connection system a bridge's performance can be performed.

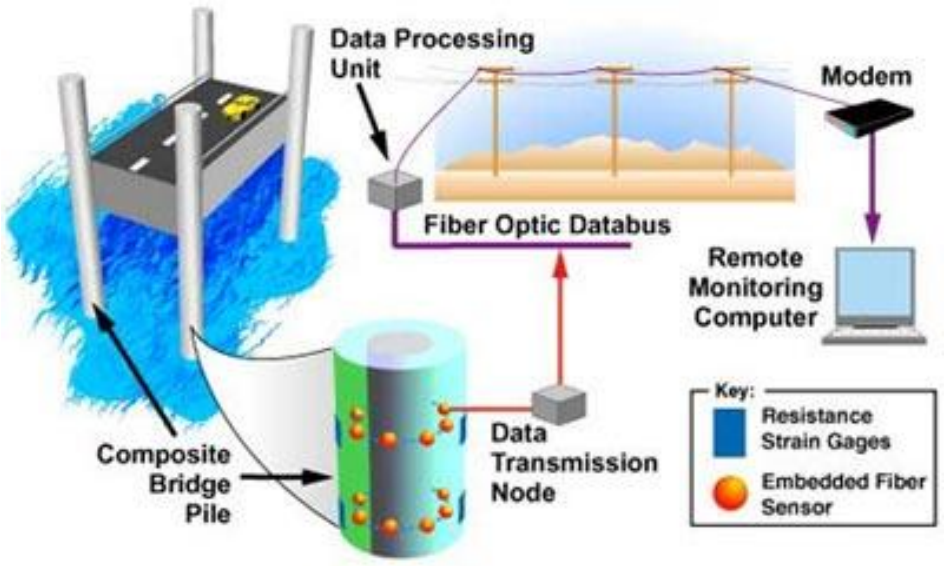

Fig. 2.2 Application of strain gauges for SHM (Problem Solving with Computers)

2.2.3 Feature Extraction

According to (Sohn *et al*., 2003) feature extraction is the withdrawal or extraction of damage sensitive parameters from the dynamic response measurement obtained from sensors. Feature extraction relies on finding the relationship between measurement responses and the observation of a system for a period of time. For example, when a structure undergoes deterioration the amount of strain developed increases through time. Therefore, one can relate strain measurement as a potential damage indicator. Other system response parameters, such as, frequency, damping ratio, and mode shape among others could be taken as a feature extraction indices due to the fact that the quantitative measurement of these parameters could indicate the progress of damage(Chen *et al*.

2004). The following sections of this subtopic try to focus on the major feature extraction methods used by different scholars for effective development of modern SHM.

2.2.3.1 ARMA/ARIMA Modal Families

Coefficients of Autoregressive Moving Average (ARMA) or Autoregressive Integrated Moving Average (ARIMA) time series models have been used in the past as a feature extraction or damage detection parameters (Carden *et al*. 2007). The rationale behind fitting time series models to a response measurement data is to detect the progress of damage through monitoring the coefficient of these models. Sohn *et al*. (2000) used coefficients of AR model in order to detect the presence of damage to acceleration response measurement obtained from a bridge column by forced excitation. The experiment was conducted in the laboratory by exciting a bridge column using actuators and electromagnetic shakers. By continuously applying a greater amount of force to the same concrete column, another set of AR modal is again fitted to acceleration response data. By observation of the coefficients of the AR modals fitted at the early and later stages of force application; the authors were able to detect the level of damage induced in to the structure. Omenzetter *et al* (2006) studied unusual events during construction and service period of a major bridge structure. In their study they showed that coefficients of the ARIMA modal fitted for the strain signal were able to detect the occurrence of unusual events. The authors showed the effectiveness of ARMA modals for damage detection. The coefficients of the ARMA modals were fed to a classifier and the classifier detected the change in the structural response of data obtained from different sources. Sohn *et al*. (2001) introduced in their study that the residuals of Autoregressive (AR) and

Autoregressive exogenous (ARX) models could be used as a feature extraction parameter. The residual the authors used was the difference between the actual measured acceleration signal and the prediction obtained using the AR modal. Mattson *et al*. (2006) introduced damage diagnosis using standard deviation of residuals after vector autoregressive (ARV) model was implemented. Other studies which used AR modal coefficients as a feature extraction can be found in Wang *et al*. (2008 and 2009).

2.2.3.2 Modal Parameters

The damping ratio is used to express how a vibration response decays after a structure is set in to motion. Most SHM systems rely on the analysis in the frequency domain. The extraction of modal parameters from sensor data is discussed in (Taha *et al.* 2006). Modal parameters of a structure include natural frequency, mode shape and damping ratio. The premise behind this methodology is that, when a structure loses its stiffness due to the application of force, the modal parameter will change and this can be detected by the application of spectral analysis tools. For healthy structures, the instantaneous natural frequency is time invariant. Peng *et al*. (2005) showed that by investigating the instantaneous frequency of a vibration response signal, obtained from a three degree of freedom (DOF) spring mass system, the loss of stiffness and hence progress of damage could be detected. When a structure, such as a bridge deteriorates due to the accumulation of damage, the natural frequency will exhibit variation instead of a constant frequency. Natural frequency can be defined as the frequency at which a structure oscillates once it is set into motion. Meo *et al*. (2006) presented the determination of natural frequencies, damping coefficients and mode shapes of a medium

span suspension bridge as feature extraction parameters by using wavelet analysis. The comparison of the extracted dynamic responses of the bridge from the displacement response data with the calculated dynamic parameters was shown to be an efficient damage indicator.

2.2.3.3 Energy Distribution

Methods which are based on the spectral analysis, which show the energy distribution of signals, are also used to identify presence of damage. Hui Li *et al*. (2009) discussed the application of marginal spectrum of a Hilbert transform to detect the progress of damage in roller bearings. Marginal spectrum measures the contribution of the total amplitude from each frequency values that exist in a signal. When damage occurs to a structure, the Hilbert energy spectrum will decrease. Furthermore, (Bassiuny *et al.*2007) discussed another application of marginal Hilbert method to fault diagnosis on a stamping process. The authors induced two types of faults during the stamping process by artificially creating a miss feed and too thick material. The strain signal obtained from the experiment is decomposed using empirical mode decomposition (EMD) and then the energy index and Hilbert transform of the signal was analyzed for detecting the induced errors in the stamping process. It is found out from the study that a change in the marginal spectrum of a response signal depicted abnormal condition on the stamping process. Energy signal under normal condition were found out to be different compared with that of the faulty conditions.

2.2.4 Statistical Model Development

Statistical model development serves the purpose of quantifying the damage status of a structure after the implementation of feature extraction. There are two major categories of statistical model development: supervised and unsupervised learning.

Supervised learning: is when response data is available from a damaged and undamaged state of a structure. Most of the time, it is not common to find data which consists of both a damaged and undamaged state.

Unsupervised learning: is the case when data is not available for the damaged state of a structure. To account for the scarcity of data from the damaged state a finite element simulation is implemented.

Statistical analysis tools are applied in a variety of studies together with both time series and frequency domain applications. A number of statistical tools have been used for the purpose of SHM up to now. Sohn *et al*. (2000) introduced the usage of one of the most widely used statistical control tools called control charts in a supervised learning manner. It is discussed in the report that after feature extraction is employed using the coefficients of AR modal; X-Bar control chart was introduced to detect the damaged and undamaged state of a bridge concrete column. The base lines of comparison, which are the control limits for the X-bar were taken from the undamaged state of the column. By constructing X-bar chart for the subsequent AR coefficients obtained from different level of damage, the authors were able to detect the outliers and hence detect the progress of damage in the concrete column. A multivariate statistical process control (MSPC) tool is applied in the study conducted by (Wang *et al*. 2008). The Hotteling T^2 chart was applied to the coefficients of Autoregressive (AR) modal, which is fitted to the acceleration

response data of a structure. The T^2 chart gave the advantage of sensitivity in the number of out of control points compared with the Shewhart x-control charts.

Fugate *et al*. (2001) applied the residual of AR (5) modal to detect damage progress. The X-bar, S-chart was used to plot and contrast the residuals of the damaged and undamaged structure. Mattson *et al*. (2006) used the standard deviation of autoregressive residual errors as a damage indicator for damage detection of roller bearings. From the results, it is shown that this residual based method standard deviation is found out to be a robust damage indicator. In this paper, it is also shown that skewness or kurtosis test used on the raw acceleration data as a damage indicator, but the outcomes were found to be unreliable. In the article by (Sohn and Farrar, 2001) it is discussed that the residual error obtained through the difference of the actual measurement and predicted modal increases as data from damaged regions is fitted. Lei *et al*. (2003)employed sum of squared difference between autoregressive(AR) coefficients and ratio of standard deviation of standard errors as a damage sensitive parameters based on data obtained from the four storey modal of ASCE task group. Other statistical tool application for damage detection, which makes use of extreme value statistics, can be found in (Park &Sohn 2006; Oh *et al*., 2009). Sohn *et al*. (2005) discussed the application of extreme value statistics for damage diagnosis on eight degree-of-freedom spring mass system. Extreme value statistics is used on data set that lies in the tails of a distribution center.

2.3 SHM Data Processing and Statistical Application

Many researchers have applied different types of data analysis techniques, which are based on the characteristics of the data acquired from the sensors. The literature review and focus of this thesis would be on signal processing methodologies used by different scholars based on the two approaches: i) Time series based SHM and ii) Frequency domain based SHM. Note that Statistical process control tools, such as control charts and PCA (principal component analysis) are used together with the above two approaches of data analysis in many of the researches that are conducted for damage diagnosis.

2.3.1 SHM-based on Time Series Analysis

The response data obtained from sensors installed on the structure is analyzed based on the different time series modeling approaches. The time series modals could be but not limited to Regression, Moving Average (MA), Autoregressive (AR), and Autoregressive Integrated Moving Average (ARIMA).

Sohn *et al*., (2000) explained the use of control charts to detect the presence of damage on a concrete column by using autoregressive (AR) modal as a feature extraction method. Feature extraction is the process of identifying parameters, which are sensitive to damage. By analyzing changes in the AR coefficients, the authors were able to predict whether the data is coming from damaged or undamaged system. In this paper, X-bar control chart is employed to monitor changes in the means of the measured data and to identify samples which are abnormal compared to data recorded previously.

Kullaa (2003) used data obtained from an actual working bridge to detect the status of damage based on the modal parameters from the response data of a bridge. The bridge used for investigation is Z24 Bridge, which is found in Switzerland. By extracting the modal parameters of the structure, such as, natural frequencies, mode shapes and damping ratio, the authors were able to detect the presence of damage. A number of univariate and multivariate control charts were used to detect the presence of abnormal characteristics based on the control limits of these control charts.

Damage identification based on time series analysis is discussed in (Omenzetter *et al*.2006). The variations in the coefficients of autoregressive integrated moving average (ARIMA) modal analyzed during the construction and service life of a bridge were used as damage indication parameter. Mattson *et al*.(2006) indicated by using one of the time series modeling approaches, which is AR model residuals to detect the existence of deterioration from data gathered from a simulation data experimented at the Los Alamos National Laboratory(LALN). From a numerically simulated case study data,(Wang *et al*., 2009) used AR modal coefficients to fit data gathered from a normal and abnormal condition of damage scenario. By using the AR coefficients together with multivariate exponentially weighted moving average control charts, the authors were able to detect whether the data is coming from a damaged state or not.

2.3.2 SHM-based on Frequency Domain Analysis

The second category of signal processing which is frequency domain based SHM is concerned with, viewing the data on hand from a different perspective i.e. spectrum analysis instead of time. The rationale behind this methodology is that information which is not readily available in the time domain could be extracted from the frequency analysis. Moreover, physical properties of structures, such as natural frequency can be easily compared with the instantaneous frequency which is obtained by this approach. The major approaches applied to date in the aspect of frequency domain are Fourier transform, Wavelet analysis and Hilbert Huang transform coupled with empirical mode decomposition (EMD). The spectral analysis method to apply in the frequency domain depends on the nature of the data acquired from the sensor system. When enough information is not readily available from the raw time series data, transformation to the frequency domain is the preferred choice. Frequency domain parameters, such as modal frequency, damping ratio and modal shapes are enormously affected when a structure is damaged. Zhu *et al*. (2008) showed that wavelet analysis successfully detected damage progress when a gradual and sudden loss is induced to the spring stiffness from a laboratory experiment of spring mass system. This loss of stiffness was depicted as a decrease in the natural frequency of the spring. Hou *et al*. (2000) discussed the application of wavelet analysis for SHM. Acceleration data obtained from simulation of simple structural modal was analyzed by using wavelet decomposition. From the details of the wavelet decomposition, the abrupt and cumulative damage progress was effectively detected.

The most recent approach among the frequency analysis methods is the Hilbert-Huang transform, which is applied together with empirical mode decomposition (EMD). The application of this method to fault diagnosis on a stamping process was discussed in (Bassinuy *et al*. 2007). The authors induced two types of faults during the stamping process by artificially crating a miss feed and too thick material. The strain signal obtained from the experiment is decomposed using EMD and then the energy index and Hilbert transform of the signal was analyzed for detecting the induced errors in the stamping process. It is found out from the study that a change in the marginal spectrum of a response signal depicted abnormal condition on the stamping process. Energy signal under normal condition was found out to be different compared with that of the faulty conditions. The application of marginal spectrum and Hilbert transform in (Li *et al*., 2007) applied on the IMF (Intrinsic Mode Function) components of the decomposed signal using EMD showed that the proposed method detected the characteristic frequency of the roller bearings faults. Yang *et al*. (2004) discussed the application of EMD and Hilbert Huang transform to detect damage time instants from data obtained on the benchmark problem from the ASCE task group on structural health monitoring. The intrinsic mode functions (IMFs) were able to capture damage spikes in the recorded data and instantaneous frequency and damping ratio were successfully obtained by using the Hilbert transform before and after damage.

According to (Pai *et al*., 2008), HHT can be used to obtain instantaneous natural frequency of bridge columns and to understand the relationship between frequency changes and bridge conditions. It is shown through experimental investigation that the wider spread the distribution of the Hilbert spectrum, the more severe damage of the

column. Natural frequency refers to the number of times a given event will happen in a second. Moreover, a progressive decrease in natural frequency indicates that a structure is deteriorating. Shinde and Hou (2004) applied Hilbert Huang transform to detect the sudden and gradual loss of stiffness by extracting the instantaneous frequency of the raw signal which was a time series data representing acceleration versus time. A simulation data obtained from the excitation of a 3 degree of freedom (DOF) spring-mass-damper system was used for analysis.

Bassiuny *et al*. (2007) used Hilbert marginal spectrum together with neural network to diagnose damage progress of a stamping process. From this study, it was found that by using Hilbert marginal spectrum as a damage indicator, the authors were able to detect damage introduced to the stamping process. A review of literature of frequency domain approaches can be found in (Pai *et al*., 2008). In this study, it is discussed that when damage event occurs during the recording period of health monitoring system, the recorded acceleration data in the vicinity of the damaged location will have a discontinuity at that time. A statistical pattern classification method based on wavelet packet transform (WPT) is developed in (Shinde and Hou, 2004) for structural health monitoring. The vibration signals obtained from a structure were decomposed in to wavelet packet components using WPT. Signal energies of these wavelet packet components are calculated and sorted based on their magnitude, from the output, the small signal energy components are discarded. The dominant component energies are defined as a novel condition index to indicate presence of damage. Results show that the health condition of the beam can be accurately monitored by the proposed method and it does not require any prior knowledge of the structure being monitored and is very

suitable for continuous online monitoring of structural health condition. It is assumed that the structure is excited by a repeated constant pulse force that might require the use of a mechanical shaker in practice.

By altering the parameters of beam elements, a damage detection strategy is presented in (Medda *et al*., 2007). Comparison between unspoiled condition of the beam with the damaged condition were made and results show that damage can be located and detected for a real vibration signal and a simulated data.

CHAPTER III

PROPOSED METHODOLOGY AND CASE STUDY

One of the challenges faced by modern SHM systems is analysis of high volume of data to characterize and detect abnormal structural behavior acquired from the sensors. Data acquired by SHM system should be managed and reduced into useable and filtered form for an SHM system to be successful (Omenzetter *et al*., 2006). One approach which has received wide application for monitoring of integrity and safety of structures based on vibration response data is time series analysis. The aim of this chapter is to apply basic concepts of the time series modeling and spectral analysis approaches for the purpose of Structural Health Monitoring (SHM).

3.1 Time Series Modeling

According to (Shumway and Stoffer,2005) time series is defined as a "collection of random variables indexed according to the order they are obtained in time."Time series modeling can be used for two basic purposes. Understanding of the behavior of the observed time series is the first one and the second is to fit a model for the purpose of predicting future values based on the past. Time series modeling assumes that a correlation exists between the observed series which is the dependence of the current

value of the series on past observed values. Time series applications have been used in a variety of fields that include economic and sales forecasting, stock market analysis, census analysis, weekly share prices, monthly profits, daily rainfall, wind speed, temperature, etc.

By using statistical tools, one can investigate if the assumption of correlation exists between adjacent points in time holds or not. Study of the nature of data is instrumental before going further to the modeling approaches. Data can be of different characteristics which might be under the categories of stationary, non-stationary, linear and non linear.

- The mean function μ_t for a random process Y_t which varies with time at (t=0,±1, ±2, ±3…)is given by Eq.(3.1) as the expected value of the series at time t.

$$\mu_t = E(Y_t) \tag{3.1}$$

- Auto covariance given by $\gamma(s, t)$ measures the linear dependence between two points on the same series observed at different times.

$$\gamma(s, t) = Cov(Y_s, Y_t) = E[(Y_s - \mu_s)(Y_t - \mu_t)] \tag{3.2}$$

where μ_s is the mean at time s and μ_t is the mean at time t. Y_s and Y_t are the time series at time s and t respectively.

- Auto correlation given by $\rho(s,t)$ measures the linear predictability of the series at Y_t based on the observed values at Y_s

$$\rho(s,t) = \frac{\gamma(s,t)}{\sqrt{\gamma(s,s) * \gamma(t,t)}} \tag{3.3}$$

- Stationary time series Y_t is a finite variance process such that
  - The mean value function μt is constant and does not depend on time and

- The covariance function $\gamma(s, t)$ depends on s and t only through their difference /s-t/.

- Partial Autocorrelation Function (PACF) : Suppose we have a time series Y_t, the partial autocorrelation of lag k is the autocorrelation between Y_t and Y_{t+k} with the linear dependence of X_{t+1} through to X_{t+k-1} removed(Box *et al.*,19 94).

- Auto Regressive (AR):is a model which is used to find an estimation of a signal based on previous output values.

$$Y(t)= \Phi_1 y_{(t-1)}+ \Phi_2 y_{(t-2)}+\ldots+ \Phi_p y_{(t-p)}+ \varepsilon_t \quad 3.4$$

where Y(t) is the current output value, $y_{(t-1)}$, $y_{(t-2)}\ldots y_{(t-p)}$ previous output values and Φ_1, $\Phi_2\ldots$ Φ_p coefficients of the AR, ε_t are white noise or error term and p is order of the AR model.

- Moving Average (MA): is a model which is used to find an estimation of a signal based on previous white noise or error term values.

$$Y(t)= \alpha_1 \varepsilon_{(t-1)}+ \alpha_2 \varepsilon_{(t-2)}+\ldots+ \alpha_q \varepsilon_{(t-q)}+ \varepsilon_t \quad 3.5$$

where $\alpha_1,\alpha_2\ldots\alpha_q$ are coefficients of MA model and ε_t ,$\varepsilon_{(t-1)} \ldots \varepsilon_{(t-q)}$ white noise observations and q is order of the MA model.

- Auto Regressive Integrated Moving Average (ARIMA): is the combination of AR and MA models with order (p,d,q). In equation (3.6) the first part is from AR and the second part indicates MA model. The d represents the number of differencing made to make the non-stationary data stationary.

$$Y(t) = \sum_{i=1}^{p}(\Phi i * Y(t-i)) + \sum_{i=0}^{q}(\alpha i * \varepsilon(t-i)) \quad 3.6$$

whereΦi and αi represents coefficients from the AR and MA models respectively.

Steps in time series analysis

i. Plot the series: to understand the behavior of the series over time and to detect if there are any underlying trends.

ii. Checking for stationarity: if the time series data is not stationary take the differencing. The differencing for a time series data X_t can be taken as $\nabla X_t = X_t - X_{t-1}$.

iii. Identification of model orders: By using ACF (autocorrelation function) and PACF (partial autocorrelation function) determined the order for the MA(moving average) and AR(autoregressive models).

iv. Parameter estimation: On the basis of ACF and PACF estimate a model for the series.

v. Diagnostic test of the model: If the time series data can be well explained by the fitted model, the residuals from the model should follow the characteristics of a white noise.

3.2 Frequency Domain Analysis

Most real life application data are time series based, that is to say, the measurement that are obtained, is a function of time. The x-axis usually represents the time elapsed and y-axis is the amplitude. One of the reasons to transform a time series signal to a frequency spectrum is to determine what frequency components exist in the time series signal. For example, the transformation of Electrocardiography (ECG) signals to frequency domain by using computerized ECG analyzers has assisted physicians to easily detect the presence of abnormal situation more easily compared with the raw signal

which initially was in time series. Time frequency analysis of signals is getting more recognition in structural health monitoring. Previously it has been used to analyze signals occurring in the fields of biomedicine, vibration analysis and telecommunications.

There are a number of signal processing methodologies which are used to transform a raw signal in time domain to frequency domain. Fourier, Wavelet and Hilbert Huang transform are the most widely used and popular methods of spectral analysis methodologies. The choice of these methods depends mainly on the nature of data to be processed. Fig.3.1 shows the spectral analysis methods to choose based on the nature of the data.

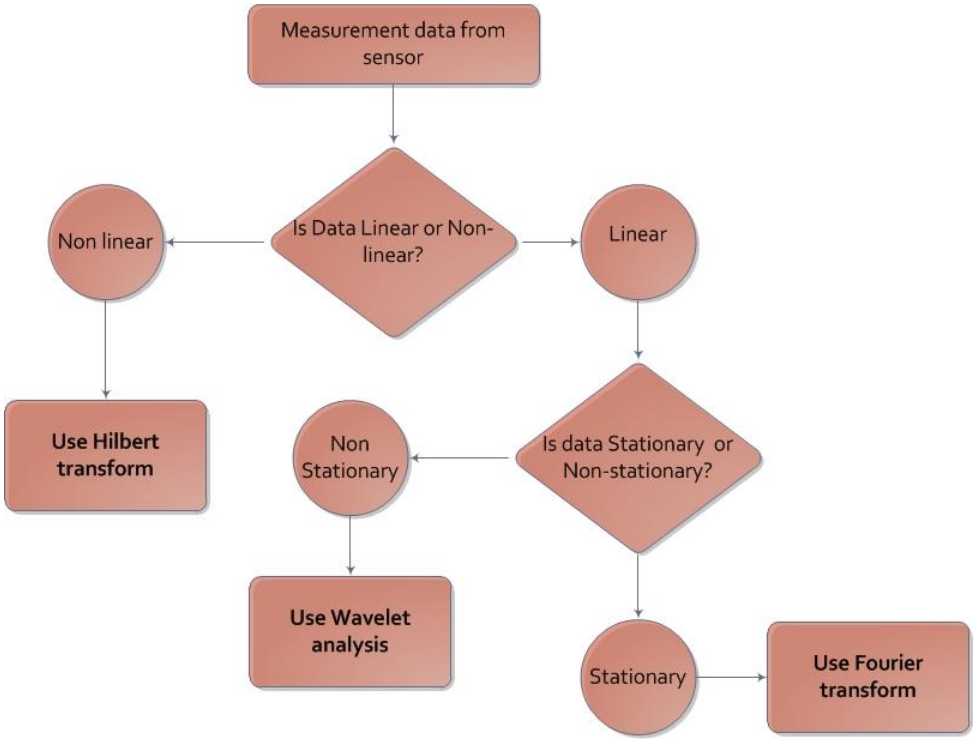

Fig. 3.1 Flow chart showing the applicability of frequency domain approaches

3.2.1 Fourier Transform

Fourier transform tells us what frequency components exist in a signal with frequency-amplitude representation which originally was a time-amplitude representation. It is utilized for stationary signals. Stationary signals have the same frequency components regardless of time, i.e. the frequency components exist at all times. Basically a Fourier transform multiply a time series signal by a sinusoidal function $e^{-2j\Pi ft}$(Polikar,2001).

$$X(f) = \int_{-\infty}^{\infty} x(t)*e^{-2j\Pi ft}\, dt \qquad 3.7$$

$$X(t) = \int_{-\infty}^{\infty} x(f)*e^{-2j\Pi ft}\, df \qquad 3.8$$

In Eq.(3.7) & Eq. (3.8) represents a raw time domain signal is represented by x(t) and X(f) is it's fourier transform. Eq. (3.8) is used to calculate the inverse fourier transform which basically is the time domain transfromation of a frequency domain signal.

Example of Fourier Transform

The following example shows the transformation of a simple sinusoidal signal in to its frequency spectrum by using the Fourier transform.

Stationary signal: Consider the sinusoidal stationary signal

x(t)= cos(2*pi*10*t)+ cos(2*pi*25*t)+ cos(2*pi*50*t)+ cos(2*pi*100*t)3.9

As shown in Eq. (3.9) the signal consists of frequency components of 10, 25, 50 and 100 Hz. From Fig. 3.4 the frequency amplitude representation of x(t) shows a peak at frequency values of 10,25,50 and 100 Hz implying the signal contains these frequency components.

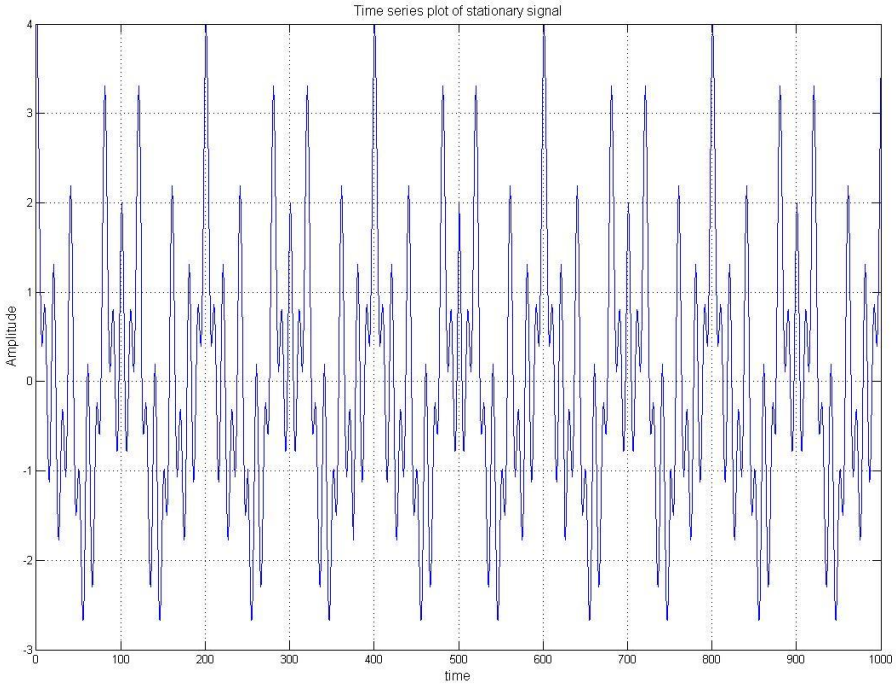

Fig. 3.2 Time series plot of stationary signal

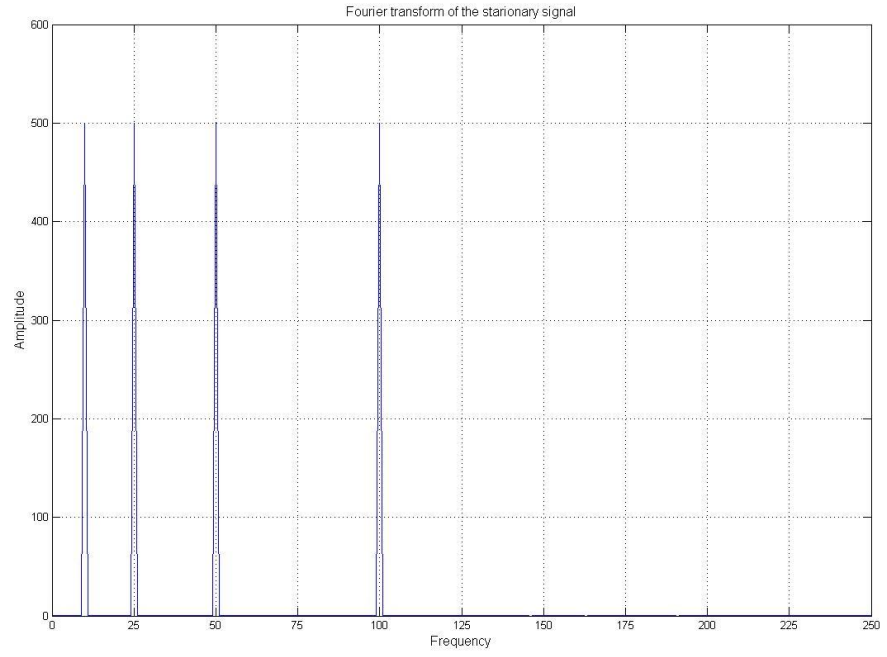

Fig. 3.3 Fourier transform of signal x(t)

The signal y (t) given by Eq.(3.10) is the sum of the signals contributed from a variety of other signals with different frequency, represents a non-stationary signal due to the fact that the frequency varies along with time (Eq.3.10). Figure 3.5 represents the time series plot of the signal y (t).

$x_1(t_1)$ = cos(2*pi*t1*100); for t1 from 0 to 0.3

$x_2(t_2)$ = cos(2*pi*t2*50); for t2 from 0.3 to 0.6

$x_3(t_3)$= cos(2*pi*t3*25); for t3 form 0.6 to 0.8

$x_4(t_4)$= cos(2*pi*t4*10);for t4 from 0.8 to 1.0

$$y(t)=x_1(t_1)+x_2(t_2)+x_3(t_3)+x_4(t_4) \qquad 3.10$$

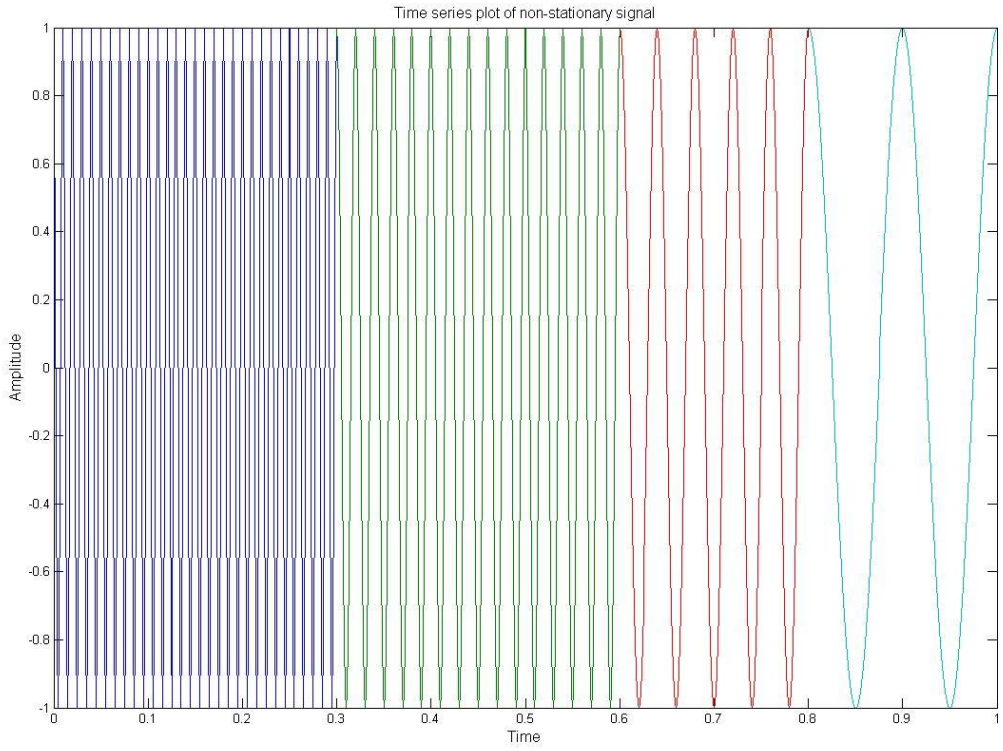

Fig. 3.4 Time series plot of signal non stationary signal y(t)

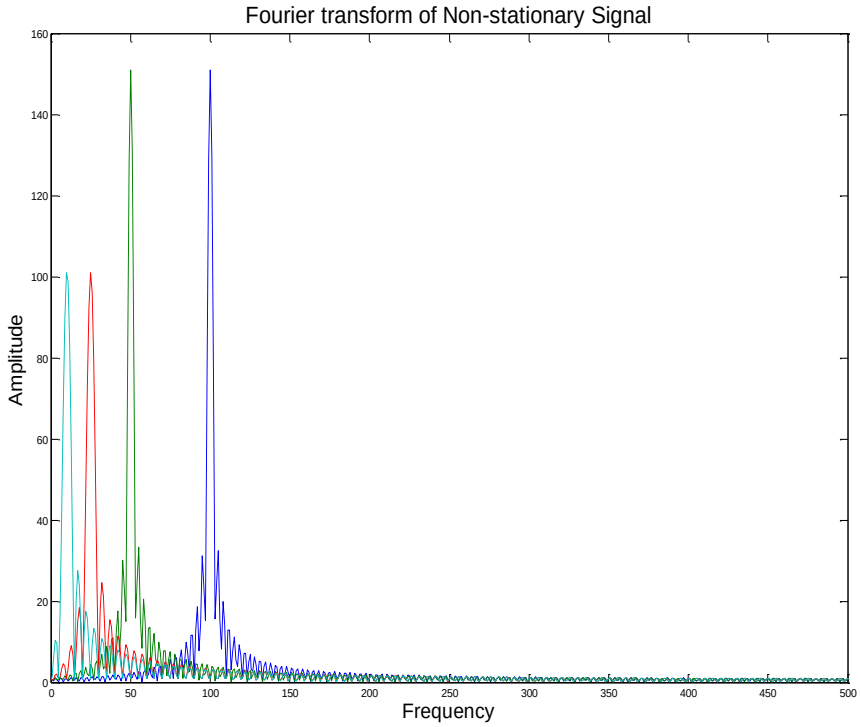

Fig. 3.5 Fourier transform of signal y(t)

The Fourier transform of y(t) shows clearly the frequency components of the signal Fig. 3.6. The amplitude of the 10 and 25 Hz frequency is lower compared to the 50 and 100 Hz because of the fact that the duration for the 10 and 25 Hz signal is less(0.2 sec) compared with the 50 and 100Hz(0.3sec). One limitation of this Fourier representation is that it does not show at what time the frequency components occur. No time information is available. From the time series plot of y(t) we can see that the higher frequency oscillations 100 and 50 Hz occurred at an early stage but this information is not shown in the Fourier transform. The Fourier transformed spectrum, provides no information on how the signal's frequency changes as a function of time for non

stationary signals. Due to this limitation of the Fourier transform a short time Fourier transform (STFT) was developed.

Short Time Fourier Transform (STFT) is developed to overcome the limitation of the lack of time information of the Fourier transform which makes use of fixed a windowing function (Polikar, 2001). STFT uses a fixed size window which moves along the signal to determine the frequency components that exist within the specified window size. The signal is assumed to be stationary within each segment of the window. From Fig. 3.4 we can see that the signal is stationary for different segments, it can be considered that the signal to be composed of four different stationary signals with a time duration of 0.3 sec (for 50 and 100 Hz) and 0.2 sec(for the 25 and 10Hz) . Once the signal is divided in to a number of window segments the next step is to apply Fourier transform to each segment of window. The difference between Fourier and STFT is that in case of STFT the signal is divided into segments of stationary parts by using a window. The width of the window is chosen where stationarity is valid for the signal under study.

The problem with STFT is resolution. We might know at what time interval the frequency existed but not exactly at what time. The window function is fixed for the entire signal which might not be the case in most application. i.e. the assumption of stationarity or width of the window is fixed at all intervals. From Fig. 3.4it is shown that the stationarity interval should vary between 0.3 sec and 0.2 sec. Usage of a very narrow window helps for the assumption of stationarity but the narrower window would not give a good frequency resolution. Therefore, there is a tradeoff between narrow window application and frequency resolution as shown on Table 3.1. On the other hand to get a perfect frequency resolution, the size of the window must be very wide or infinite in case

of Fourier transform. In Fourier transform there is no problem of identification of what frequency components exist but there is no time indication which means we have a zero time resolution. In case of a raw time series signal the value of the signal at any time is known but no frequency information can be obtained, i.e., it is a zero frequency resolution.

Table 3.1 Relationship between time resolution and frequency resolution in STFT

Window Size	Time resolution	Frequency resolution
Narrow window	Good time resolution	Poor frequency resolution
Wide window	Good frequency resolution	Poor time resolution

3.2.2 Wavelets Transform

Wavelet analysis is the decomposition of a signal in to shifted and scaled versions of the original wavelet. It is developed to overcome the fixed size window analysis of the Short Term Fourier Transform. Wavelet can be defined as a small wave extending over a finite time duration unlike cosine and sine waves which extends from minus to plus infinity in case of Fourier transforms(Pokilar,2001).

Let x(t) be the signal to be analyzed or to be transformed in to a frequency domain. The mother wavelet is chosen to serve as a prototype for all windows in the process. All the windows that are used are the dilated (or compressed) and shifted versions of the mother wavelet. As shown in Eq. (3.11), (Hou *et al*., 2000), the transformed signal is a function of two variables, a and b: the translation and scale parameters, respectively.

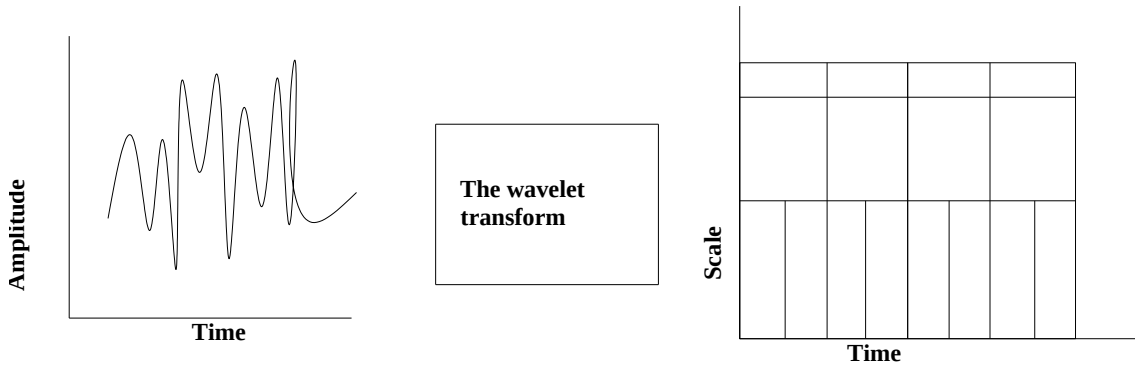

Fig. 3.6 The wavelet transforms process (Zemmour, 2006)

$$\text{CWT}(a,b)=\frac{1}{\sqrt{a}}\int_{-\infty}^{+\infty} x(t) * \Psi\left(\frac{t-b}{a}\right)dt \qquad 3.11$$

where Ψ(t)is the mother wavelet and CWT is the continuous wavelet transform which is given as a function of the coefficient of the scaled and translated form of the mother wavelet. The higher the wavelet coefficient the more resemblance between portion of the raw signal and the mother wavelet chosen.

Instead of frequency the term scale is used in wavelet analysis. The scale works as in the same way with the scale of a map. A lower scale shows a compressed size of the map while a higher scale represents detailed contents of the map. Lower scale corresponds with higher frequency and vice versa (Bayissa *et al*., 2007). Wavelet analysis can be either continuous or discrete. Discrete wavelet is used for signal decomposition and continuous wavelets are used for spectral analysis. In Fig. 3.7 the ‘s’ represents scale and ‘f’ is frequency. As the scale decreases, the frequency increases. By comparing the

signals when s=1 and s=0.05 it can be seen that the frequency is highest (f=20) when the scale is lowest(s=0.05).

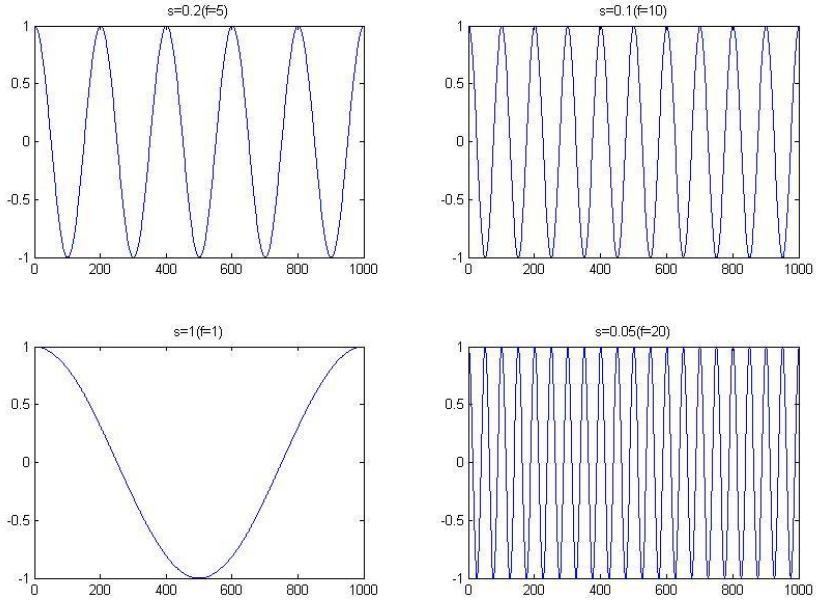

Fig. 3.7 Relationship between scale and frequency in wavelet transform

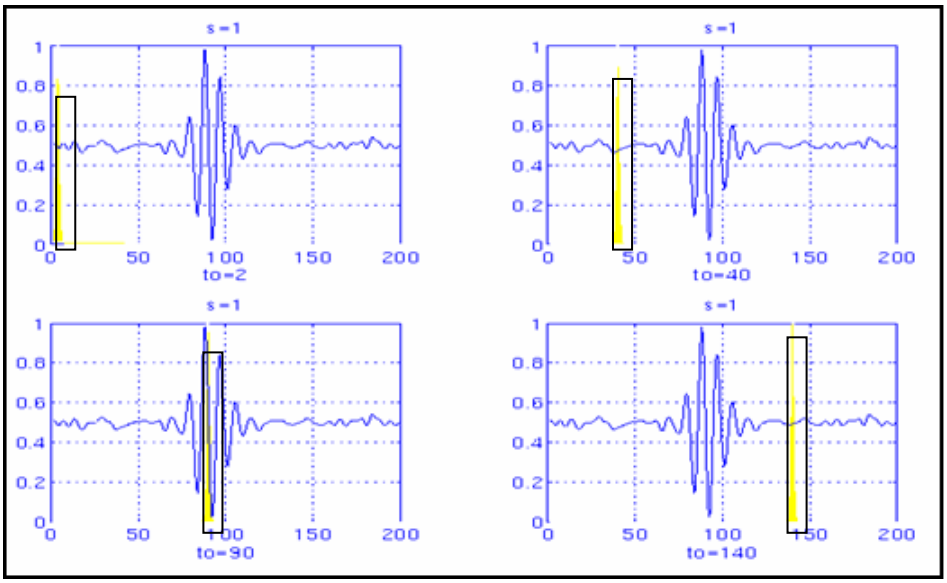

Fig. 3.8 Translation of a mother wavelet along a signal for a s=1(Polikar, 2001)

In wavelet analysis translation is moving the mother wavelet across the signal for each scale that is considered. From Fig.3.8 at a scale of (s=1), the window or the mother wavelet continuously moves along the time axis. Four different location of the wavelet is shown when it is at 2sec, 40sec, 90sec, and 140 sec, respectively. The whole signal is multiplied by each scale at different locations as in Eq. (3.9) of the mother wavelet and a higher value indicates that the signal contains more of the attributes of the multiplying wavelet.

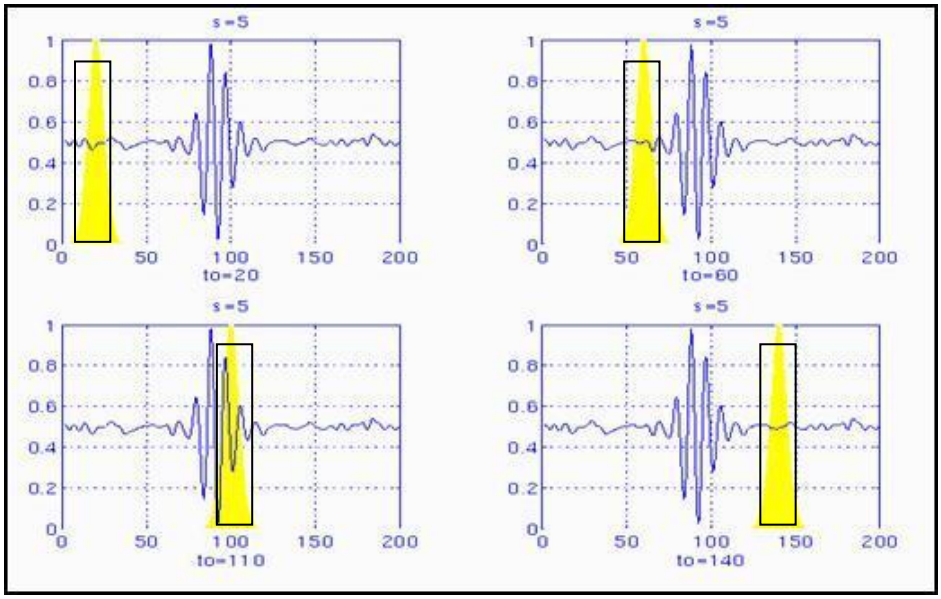

Fig. 3.9 Translation of a mother wavelet along a signal for a s=5 (Polikar, 2001)

As illustrated in Fig. 3.9 the scale of the wavelet has increased from s=1 to s=5 (lower frequency mother wavelet) compared to Fig 3.8. The signal is multiplied by this scale at different positions, and it will pick up the lower frequency components of the raw signal.

The goal in Wavelet transform is to turn the information of a signal into numbers which are coefficients that can be manipulated, stored, transmitted, analyzed or used to reconstruct the original signal (Zhu *et al*., 2007). Wavelet transform is aimed at converting information contained in a time-series signal in to wavelet coefficients so that one can detect changes in the analyzed and transformed coefficients which might be hidden in the raw time series signal. These coefficients can be represented in a graphical representation called scalogram. A scalogram is time (translation)-scale (frequency) representation of a transformed signal where a coefficient is computed for each combination of scale and translation. The color intensity represents the wavelet coefficients. A bright color corresponds to a higher wavelet coefficient; this in turn represents a strong correlation between the signal and the wavelet applied (Pokilar, 2001). Therefore a strong correlation or higher wavelet coefficient or brighter color intensity means that a portion of the signal resembles the wavelet.

3.2.3 Hilbert-Huang Transform(HHT) and Emperical Mode Decompositon(EMD)

3.2.3.1 Hilbert Huang Transfrom(HHT)

HHTtakes a function u(t) as an input and produces a function, H(u)(t), with the same domain. Hilbert transform has got a wide application for data which are non-stationary and non-linear (Huang and Attoh-Okine , 2005).

$$H(u)(t) = p.v. \int_{-\infty}^{\infty} u(T)h(t-T)dT = 1/\pi \int_{-\infty}^{\infty} (\frac{u(T)}{(t-T)})dT) \qquad 3.12$$

where H(u)(t) is the Hilbert transform of u(t), and u(t) is any real valued function, p.v. is the principal value of the singular integration.

Hilbert transform can also be described by the equation,

$$z(t)= x(t)+j\ y(t) = a(t)\ e^{j\theta(t)} \quad 3.13$$

where a(t) is the instantaneous amplitude and is given by

$$a(t) = \sqrt{x(t)^2 + y(t)^2} \quad 3.14$$

$\theta(t)$is the phase function and the phase angle from which the instantaneous frequency is calculated as given by Eq. (3.7) and Eq.(3.8).

$$\omega(t) = \frac{d\theta(t)}{dt} \quad 3.15$$

$$f= (1/2\pi) \left(\frac{d\theta(t)}{dt}\right) \quad 3.16$$

One advantage obtained with the representation in Eq. (3.16) is that frequency can be determined at any given time t, since frequency can be calculated by differentiating the phase angle with respect to time (Huang and Attoh-Okine, 2005).

The following example illustrates the effect of having a zero mean in the application of Hilbert transform. All the three functions are the same sinusoidal function except for mean shifted by 0.5 and 1.5 as shown in Fig.3.10.

Example on Hilbert transform: Consider three signals given by a =sin x +α, for α = 0, 0.5, 1.5 from which we can have three different sinusoidal signals: sin x, sin x+0.5 and sin x+1.5 (Huang and Attoh-Okine, 2005).

The first step in the extraction of instantaneous frequency is transformation of the signal by using Hilbert transform to obtain the phase plane diagram inFig.3.11. From the plane or phase diagram, phase angle is withdrawn as depicted in Fig.3.12 by differentiating the phase angle with respect to time and instantaneous frequency is obtained using Eq. (3.16).

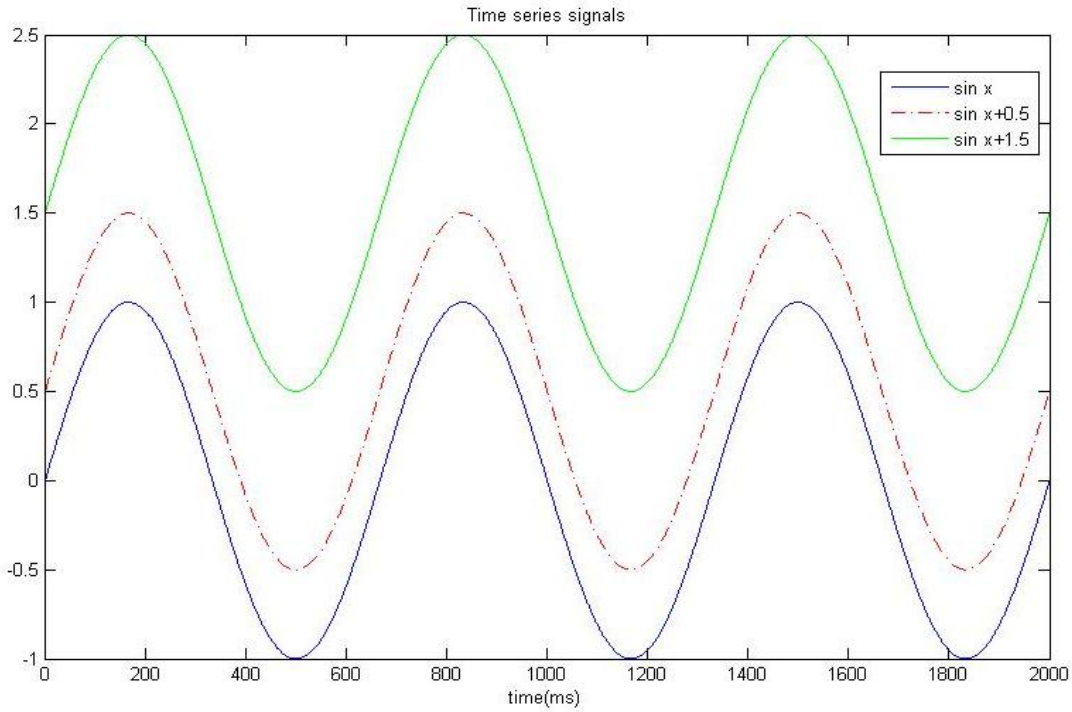

Fig. 3.10 Time series plots of signals of sin x +α, for α =0, 0.5, 1.5

From the three sinusoidal plots of the three signals with identical shape but different mean values, it is obtained that the frequency is positive and constant for the signal (sin x) with zero mean as shown in Fig.3.13. For the (sin x+ 0.5) signal the frequency is not constant and for the third signal which is (sin x +1.5) the frequency fluctuates between negative and positive values.

This example shows that the instantaneous frequency gives a meaningful value when a signal such as a sine function is symmetrical with respect to the zero mean. Therefore, to obtain Hilbert transform and hence instantaneous frequency, the raw signal should have a mean value symmetrical with respect to zero. To accomplish this purpose, a signal should be analyzed using Empirical Mode Decomposition (EMD) prior to applying the Hilbert Huang transform.

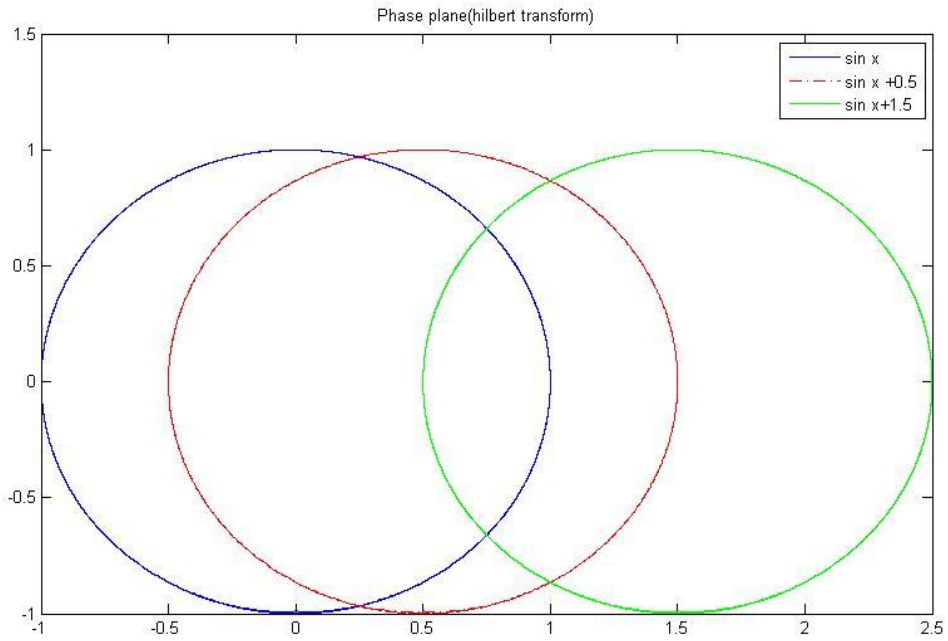

Fig. 3.11 Hilbert transform of sin x+ α for α =0, 0.5, 1.5

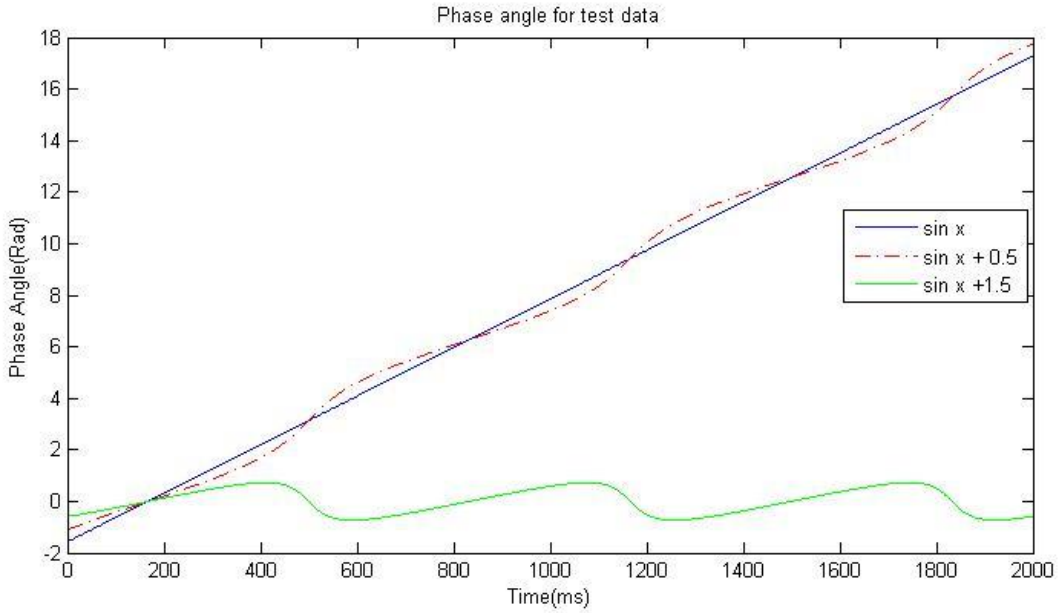

Fig. 3.12 Phase angle of sin x+ α for α =0, 0.5, 1.5

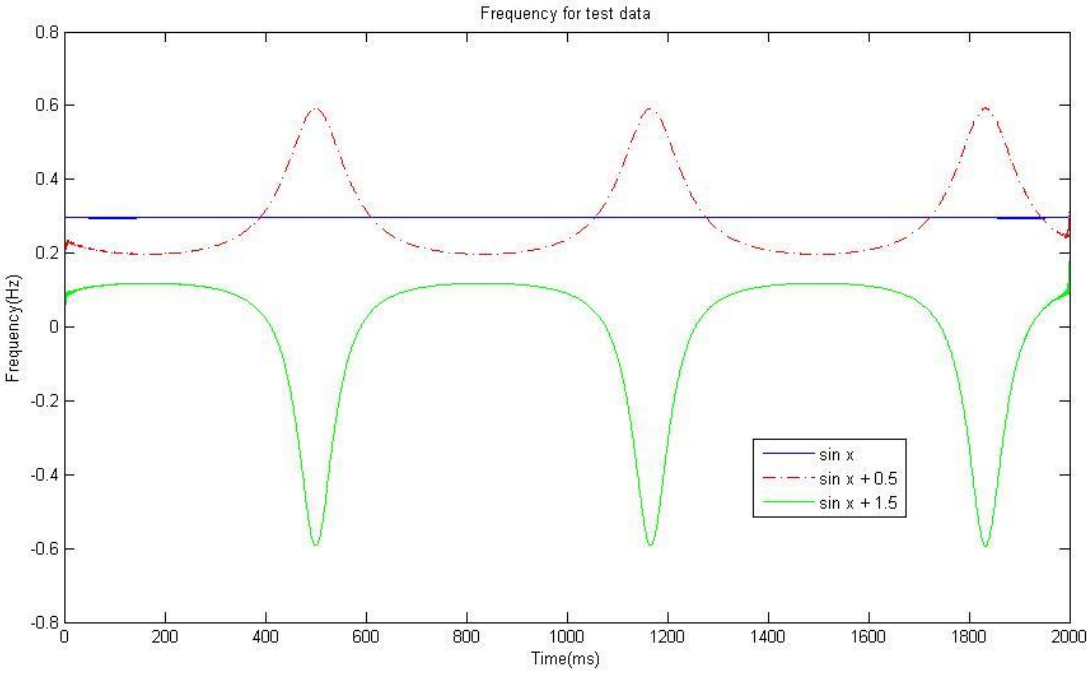

Fig. 3.13 Instantaneous frequency of sin x+ α for α =0, 0.5, 1.5

3.2.3.2 Empirical Mode Decomposition (EMD)

EMD is a fundamental and is a necessary step to reduce any given data in to a collection of intrinsic mode functions (IMF) to which the Hilbert analysis can be applied (Huang and Attoh-Okine, 2005). An IMF represents simple oscillatory mode embedded in the raw data where each IMF deals with only one mode of oscillation with no complex riding waves present. Since most data does not represent IMF naturally the Hilbert transform is not capable of producing full description of frequency if the data contains more than one oscillatory mode at a particular time. Due to this reason, data should be decomposed in to independent IMF components.

Sifting is the process of decomposition of a signal in to its IMF components by using Empirical Mode Decomposition (EMD). The sifting process can be explained by the following steps.

Step1. Assume a signal x(t) is given to be sifted by EMD. Find all the upper and lower peak points of the signal and create upper and lower envelop by interpolation. The upper envelop can be denoted by emax(t) and the lower by emin(t) and take the average of the envelopes emax(t) and emin(t) to get m1Fig. 3.15a.

Step 2. Subtract the envelope mean m1 from the original signal. This is shown on Fig.3.15b as h1=x(t)-m1.

After this step check if the new data h1 has fulfilled the criteria for IMF or not and if h1 is not IMF, repeat the steps given by 1 and 2.

The criteria for a sifted signal to be IMF is

i. When number of extrema(maxima+minima) and zero crossings are the same or differ by one and

ii. Envelopes as defined by all the local maxima and minima are being symmetric with respect to zero (Huang et el. 2005).

The sifting process should stop when the SD (standard deviation) between two consecutive sifted signals is smaller than a preset value given by Eq.(3.14).The original signal(data) to be sifted x(t) can be represented by Eq. (3.15) which illustrates the decomposition of x(t) in to n-IMF components(Cj) and a residue(r_n).

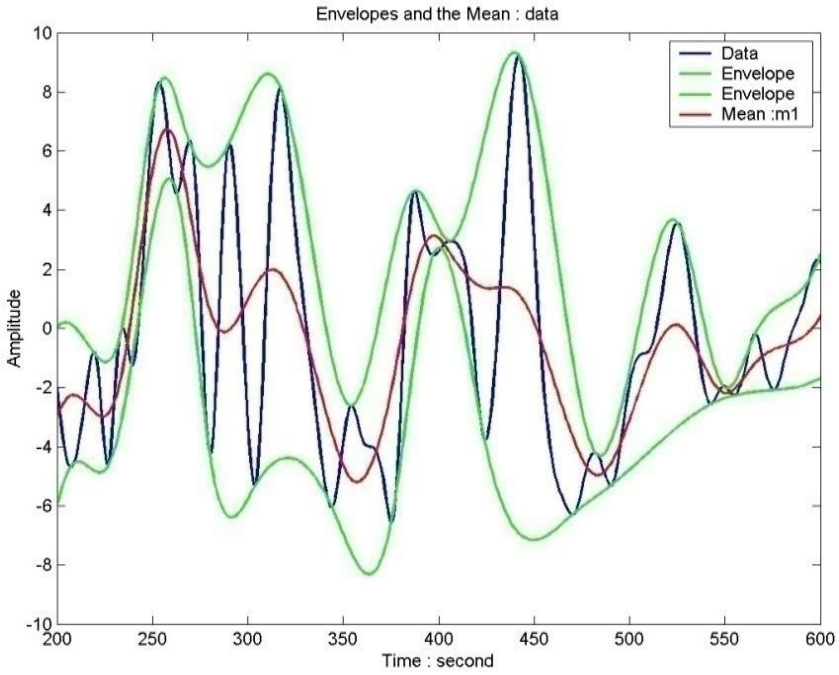

Fig. 3.14(a) The cubic spline upper and the lower envelopes and their mean h1 (Huang and Attoh-Okine, 2005)

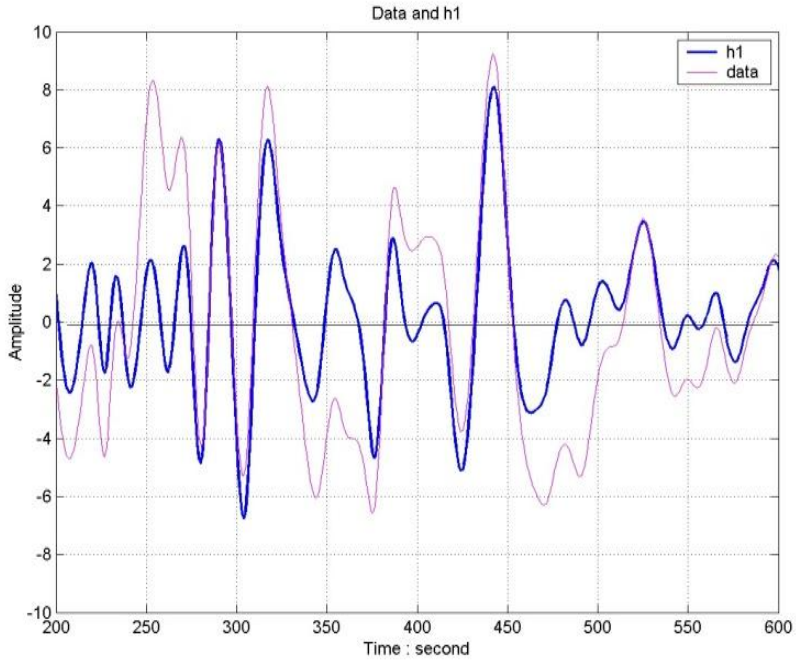

Fig. 3.14(b) Comparison between data x(t) and h1 (Huang and Attoh-Okine, 2005)

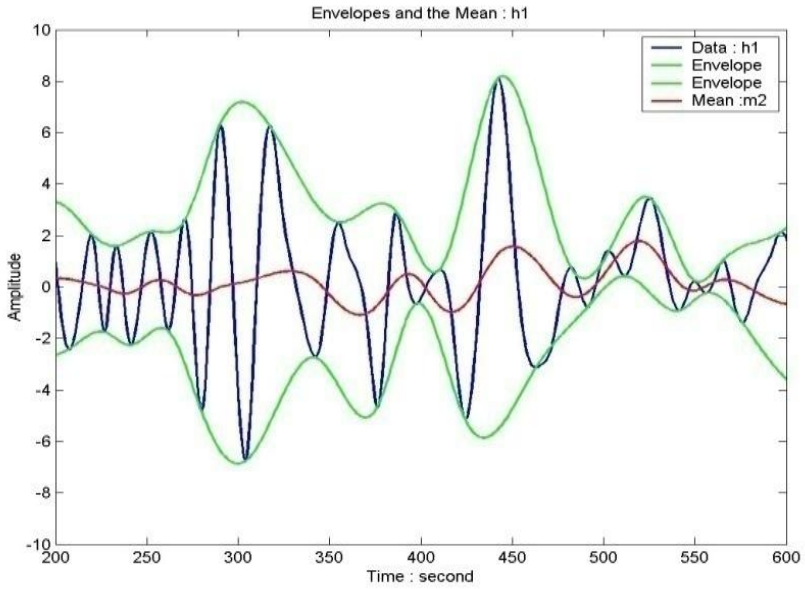

Fig. 3.14(c) Repeat the sifting process using h1 as data
(Huang and Attoh-Okine, 2005)

In Eq.(3.14) $\left(h_{1(k-1)}(t) \text{ and } h_{1k}(t)\right)$ represents two consecutive sifted signals. The residual r_n, can be either a constant, monotonic mean trend or a curve having only one extrema point.

$$SD = \sum_{t=0}^{T} \frac{\left(h_{1(k-1)}(t)+h_{1k}(t)\right)^2}{h_{1(k-1)}(t)^2} \qquad 3.17$$

$$x(t)= \sum_{j=1}^{n} Cj+r_n \qquad 3.18$$

IMFs have are always symmetrical with respect to the local mean and have a unique local frequency different from the rest of the other IMFs. Fig. 3.15 summarizes the steps to be followed in the EMD sifting process in the form of a flow chart.

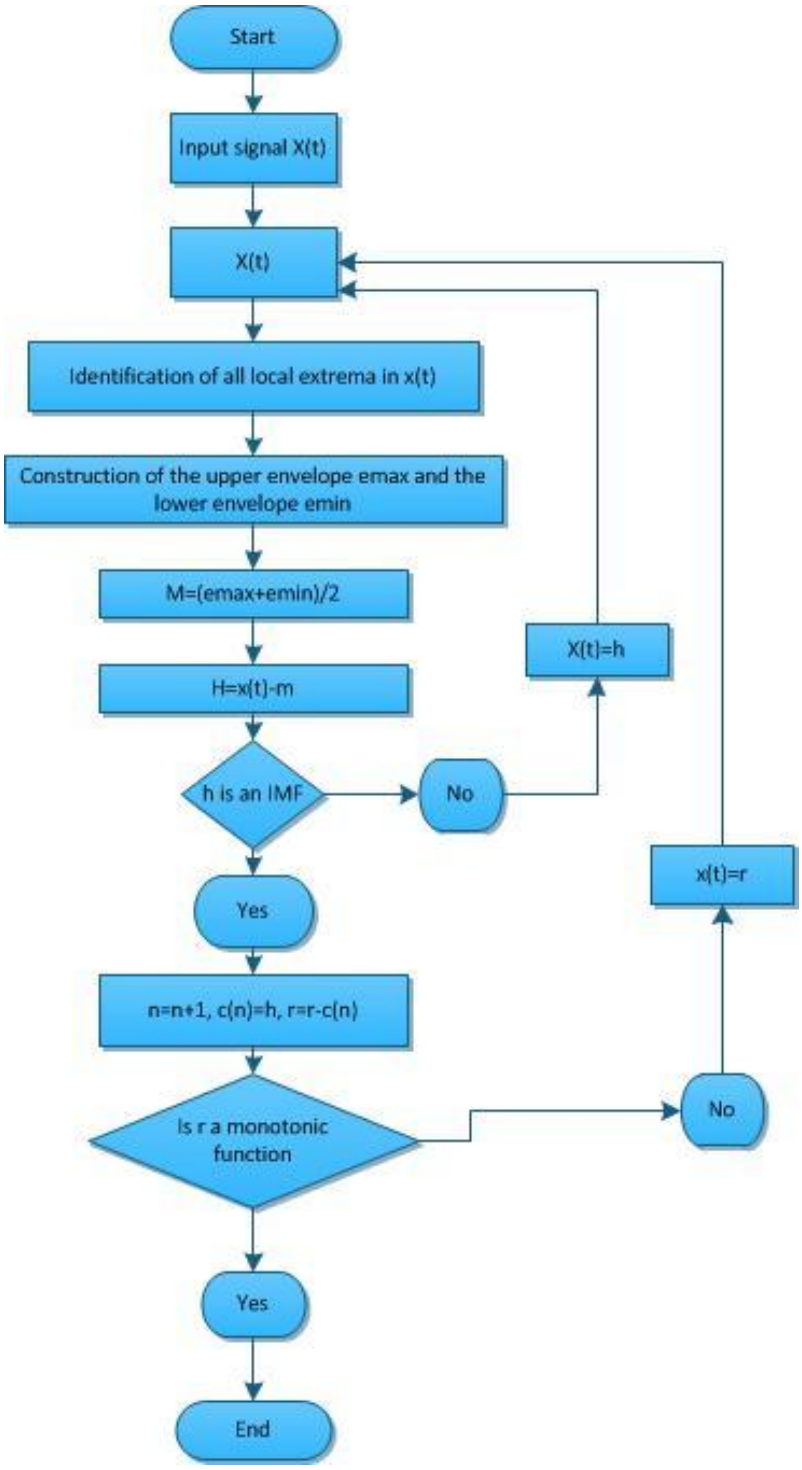

Fig. 3.15 Flow chart showing the steps in EMD (Zemmour, 2006)

3.2.4 Comparison of Fourier, Wavelet, and Hilbert Transform

For the purpose of comparison consider a chirp signal which changes frequency continuously with time.

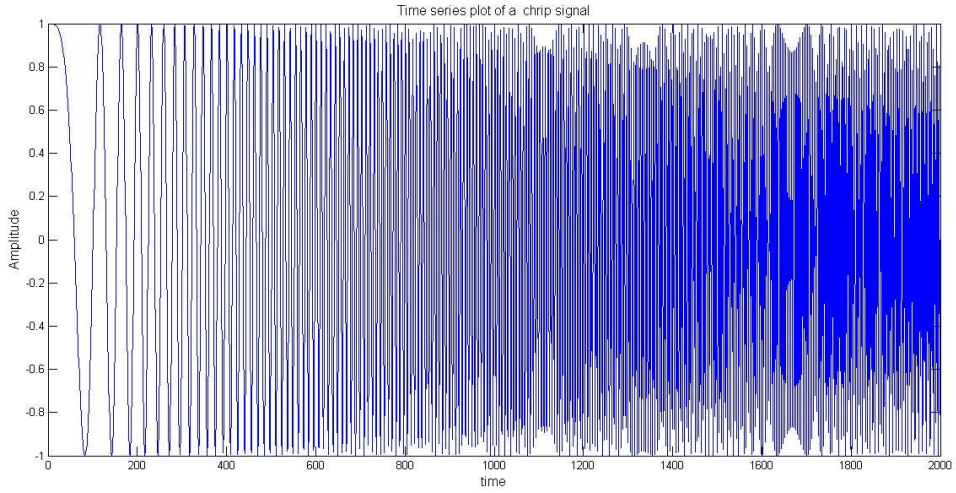

Fig. 3.16 Time series plot of a chrip signal

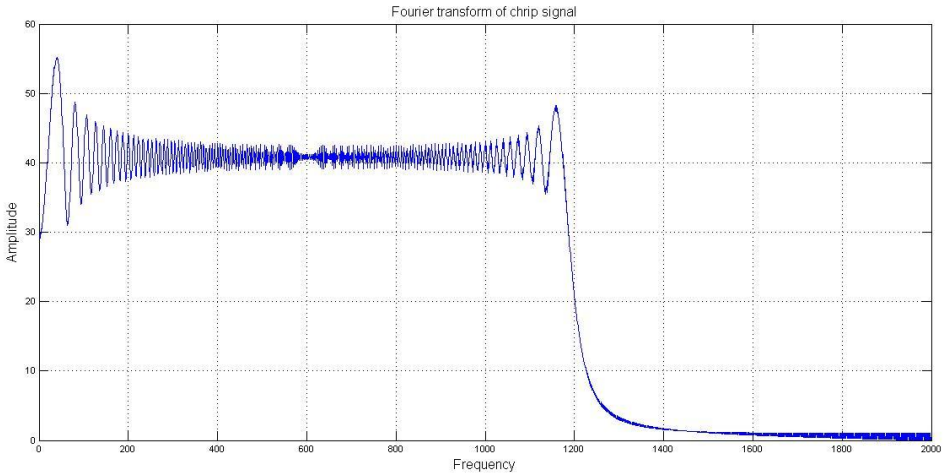

Fig. 3.17 Fourier transform of chrip signal

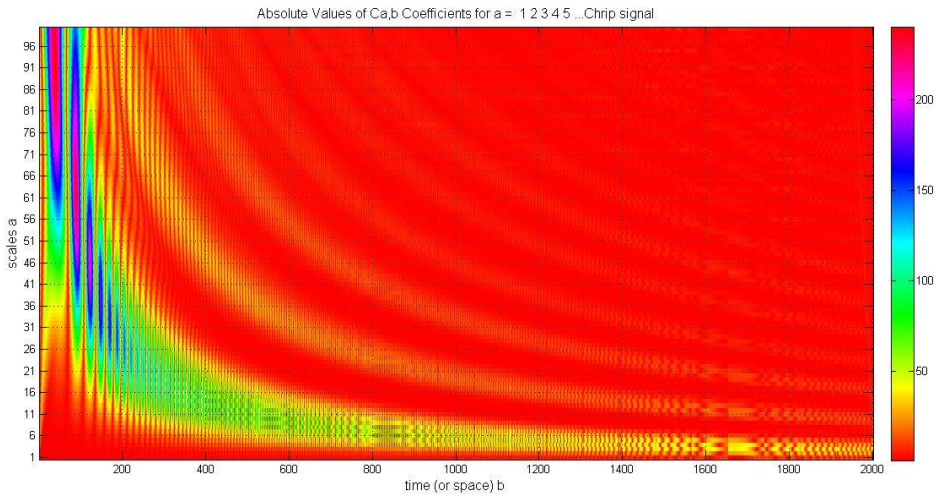

Fig. 3.18 Continuous wavelet transform of the chrip signal

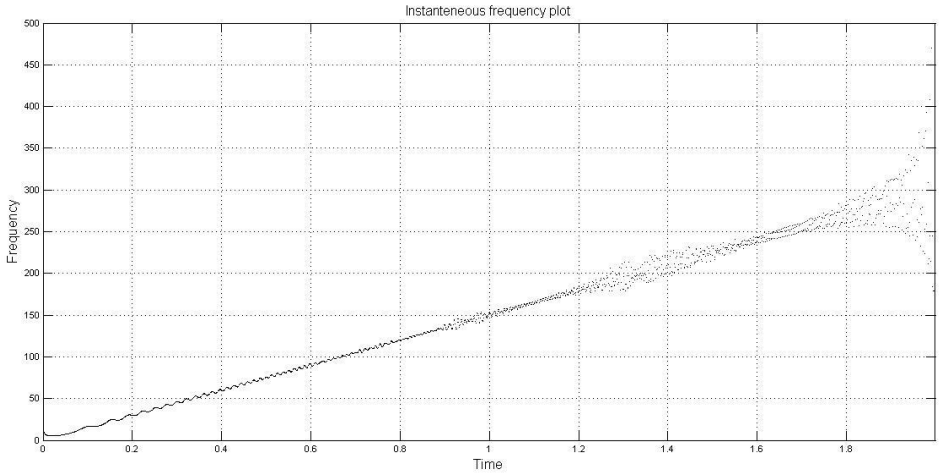

Fig. 3.19 Instantaneous frequency plot of the chrip signal

The Fourier transform of the chrip signal Fig 3.17 shows the high frequency components with a horizontal line with no information at what time the frequencies occur. The spectrogram in Fig. 3.19 illustrates graphically that the low frequency components of the signal occur at an early stage by indicating it with higher scale values. The scale of bright line goes decreasing through time in the spectrogram implying an increase in frequency since a decrease in scale represents an increase frequency. Whereas

the instantaneous frequency Fig. 3.19 which is the product of Hilbert transform demonstrates that the frequency increases constantly with time. One advantage of this representation over the continuous wavelet transform is that, the frequency at the desired instant of time can be obtained.

Therefore Hilbert transform looks the favorite candidate among the spectral analysis tools. Table 3.3 revises the advantage and disadvantages of the three frequency domain approaches.

Table 3.2 Comparison between the different frequency domain analysis methodologies

	FOURIER	WAVELET	HILBERT HUANG
Basis	A priori	A priori	Adaptive
Frequency	Convolution: global, uncertainty	Convolution: Regional, uncertainty	Differentiation: local, certainty
Presentation	Energy-frequency	Energy-time-frequency	Energy-time-frequency
Non linear	No	No	Yes
Non Stationary	No	Yes	Yes
Feature extraction	No	Discrete: No Continuous: yes	Yes

CHAPTER IV

IMPLEMENTATION OF PROPOSED METHOLOGIES

4.1 Data Sources for Analysis

In order to validate the proposed methodologies of data analysis tools, simulation data and data from a functional (working) bridge were applied. This chapter explains the application of the proposed methodologies, to data sources obtained from two different sources. Spectral analysis of a benchmark problem simulation data is presented in the first section followed by statistical analysis and time series modeling for the bridge data.

4.1.1 Data Source from Bridge

For the purpose of time series analysis data was obtained from strain gauge sensors installed on a bridge found in Texas. Four sensors were mounted on two of the supporting columns of the bridge since 2001. Apart from deformation measurements, temperature at each of the sensors was also measured by the strain gauge sensors. The data obtained contains three years full data from 2002-2004 and partial year data for year 2001 and 2005 measured every hour of a day.

Fig. 4.1 Supporting column of the bridge

4.1.2 Data Source from Simulation

Data obtained from a 4-storey and 2-bay by 2-bay steel frame scale model structure as shown in Fig. 4.2 designed by theAmerican Society of Civil Engineers(ASCE) for the purpose of SHM was gathered to show validity of the spectral analysis approaches. The structure is located in the earthquake engineering research laboratory at the University of British Colombia (UBC) (Johnson *et al*., 2004). In this

study to excite the structure the cases considered were electrodynamic shaker,impact hammer, and ambient excitation.

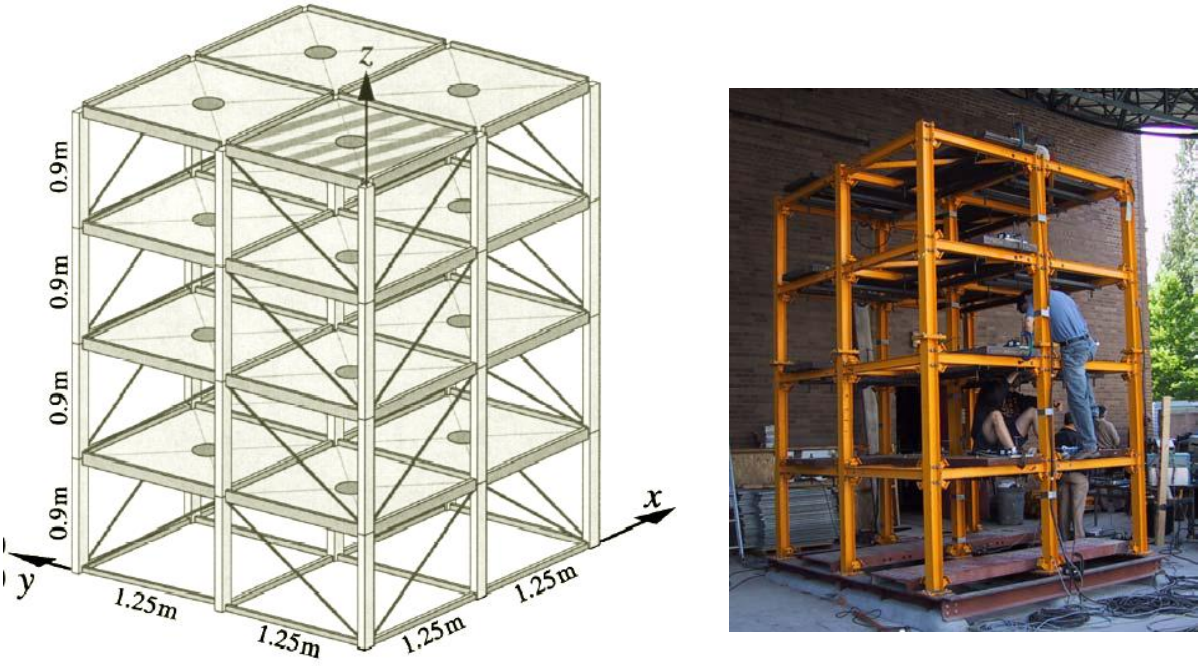

Fig. 4.2 Picture and 3D model showing the bench mark problem building (Johnson *et al*., 2004)

For the electrodynamics shaker excitation, the shaker was placed on top floor the structure with a capacity of 311 N (Dyke *et al*. 2003). To capture the response of the structure accelerometers were placed throughout the structure in the structure's weak(y-direction) and strong (x-direction). Based on the experiments conducted in the earthquake laboratory, a Matlab algorithm by the name 'DATAGEN' was developed to simulate the real conditions of the experiment (Lin *et al*., 2005).

4.2 Frequency Domain Analysis of Simulation Data

The bench mark structure from which simulation data was taken is a 2.5 m by 2.5m floor area and 3.6 m high Fig. 4.2. A bracing system placed along the diagonal was fixed for each bay and to emulate a real structure a concrete slab was built at each floor and the removal of these braces is designed to simulate damage to the structure. For the experiment wind ambient excitation and another two types of forced excitation sources were introduced (Dyke *et al*., 2003). Impact hammer test and electrodynamics shaker were applied for the forced excitation case. A more detailed description of the bench mark structure problem can be found in (Johnson *et al*., 2004). One undamaged case and six damage patterns were the subject of study of this benchmark problem. Matlab code by the name 'DATAGEN' is used to run the simulation according to the damage patterns shown in Table 4.1 and Fig. 4.3.

Table 4.1 Damage patterns and their description considered in the Matlab program (Johnson *et al*., 2004)

Damage case	Description(method of execution)
Pattern-1	Removing all the braces in the 1st floor
Pattern-2	Removing all the braces in the 1st and 3rd floor
Pattern-3	Removing one brace in the 1st floor
Pattern-4	Removing one braces from both the 1st and 3rd floor
Pattern-5	Removing one braces from both the 1st and 3rd floor plus one of the beams partially unscrewed from the column
Pattern-6	Area of one brace in the 1st floor reduced to 2/3

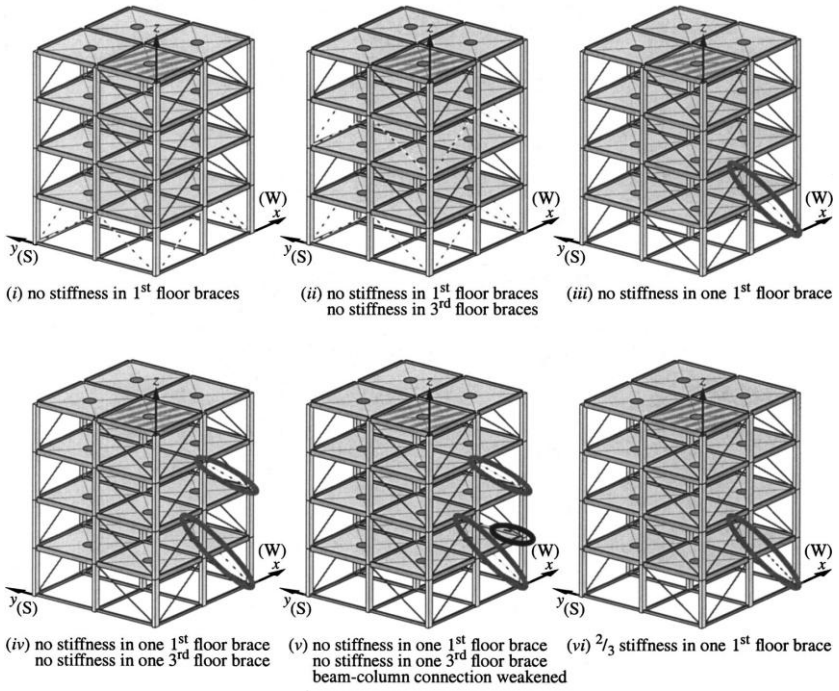

Fig. 4.3 Six damage patterns defined by the Benchmark problem (Johnson *et al*., 2004)

The six damage patterns used for the simulation are revised in Table 4.1. Fig. 4.4 explains the each damage patterns graphically. Table4.2 summaries four different cases considered for demonstration of the spectral analysis approaches obtained by applying the Matlab program (DATAGEN) provided by the study group, (Lam, 2000).

Four different cases were devised to test the validity of the frequency domain approaches. The first one is data withdrawn from the undamaged state of the structure by applying the default parameters of the Matlab program. The second case is obtained by running the simulation for damage pattern-2 which is removing all the braces from the 1st and 3rd floor. The third case considered is data from damaged condition but with a less damage extent (pattern-1) simulated by removing the braces on the 1st floor as shown in

Table 4.2 Different damage scenarios considered

Case	Damage status	Damage pattern
1	Undamaged	Undamaged(No braces removed)
2	Damaged	Removing braces 1st and 3rd floor
3	Damaged	Removing braces from 1st floor
4	Mixed cases	Combination of case-1 and case-2

Table 4.2. Case-4 is the combination of damaged (pattern-2) and undamaged conditions of the bench mark structure. There were 4 accelerometer sensors installed on each floor of the structure (Lam, 2000).

The sampling frequency taken for all the different cases is 1000Hz and the time span of the simulation is 40 sec. In this study simulation data from the 4th floor were considered. The time series plot, the Fourier transform and, 2D&3D wavelet plots are presented in the following sections.

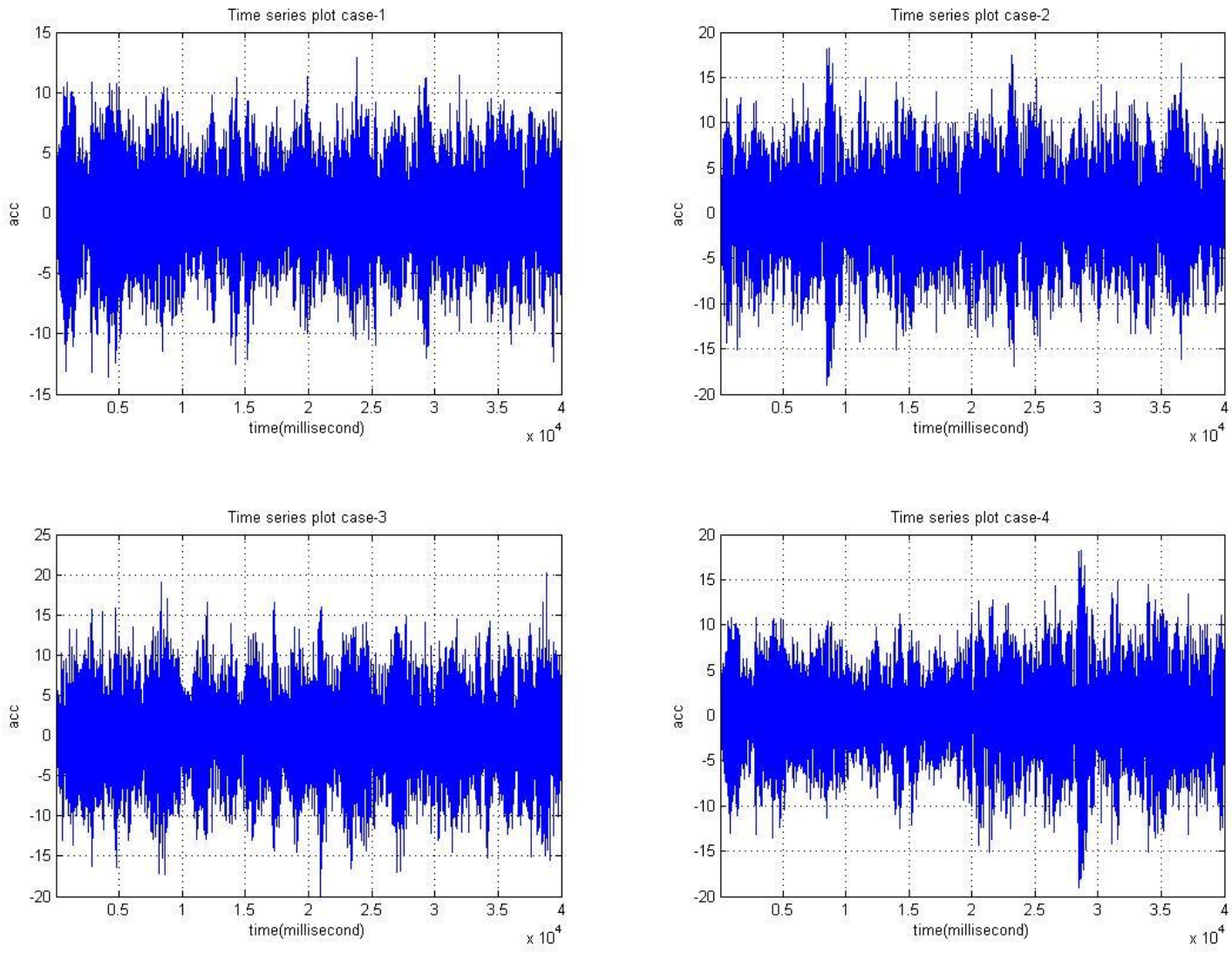

Fig. 4.4 Time series plot of the damage scenarios considered (case1-case 4)

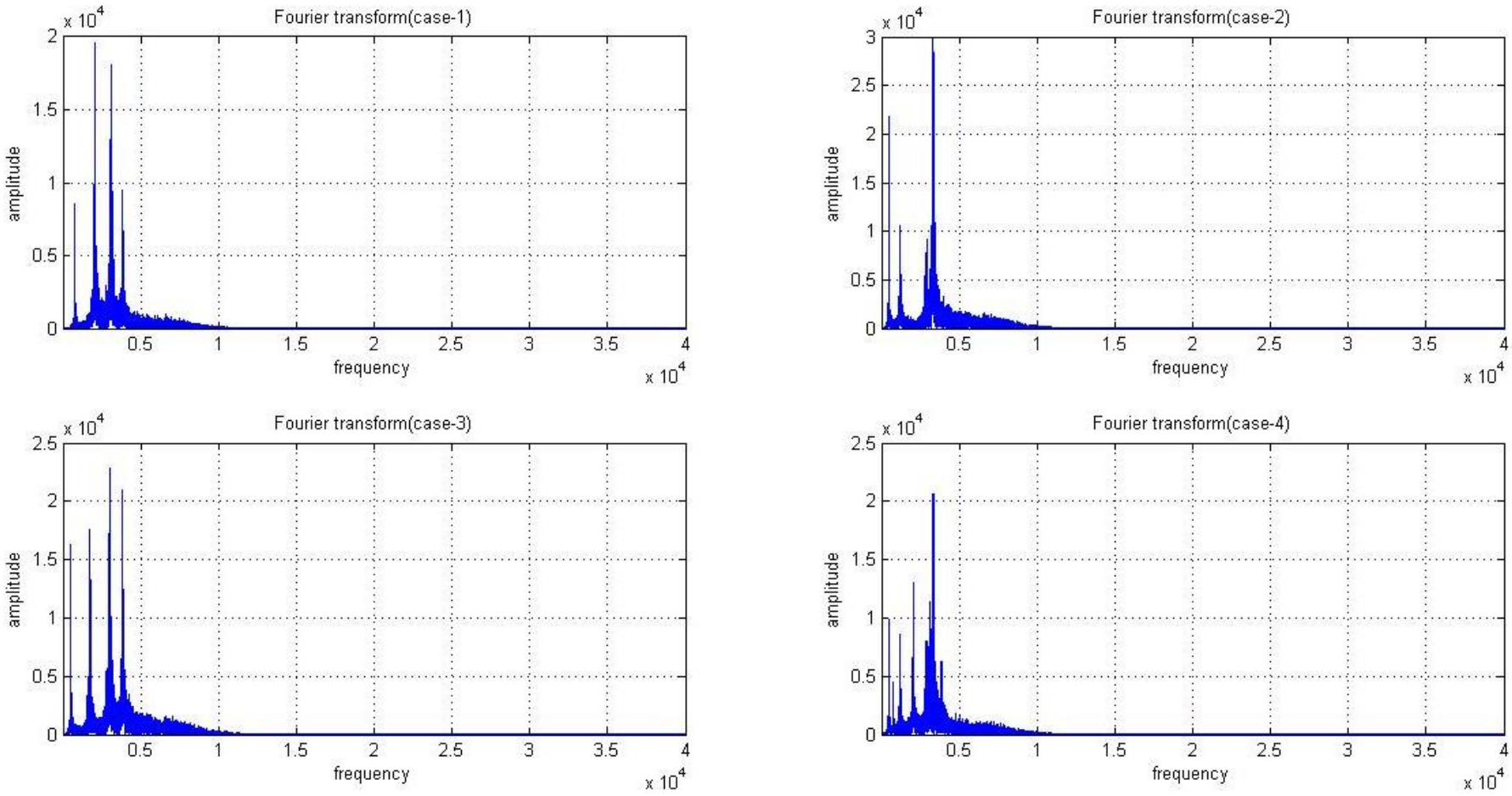

Fig. 4.5 Fourier transform of the four cases (case1-case 4)

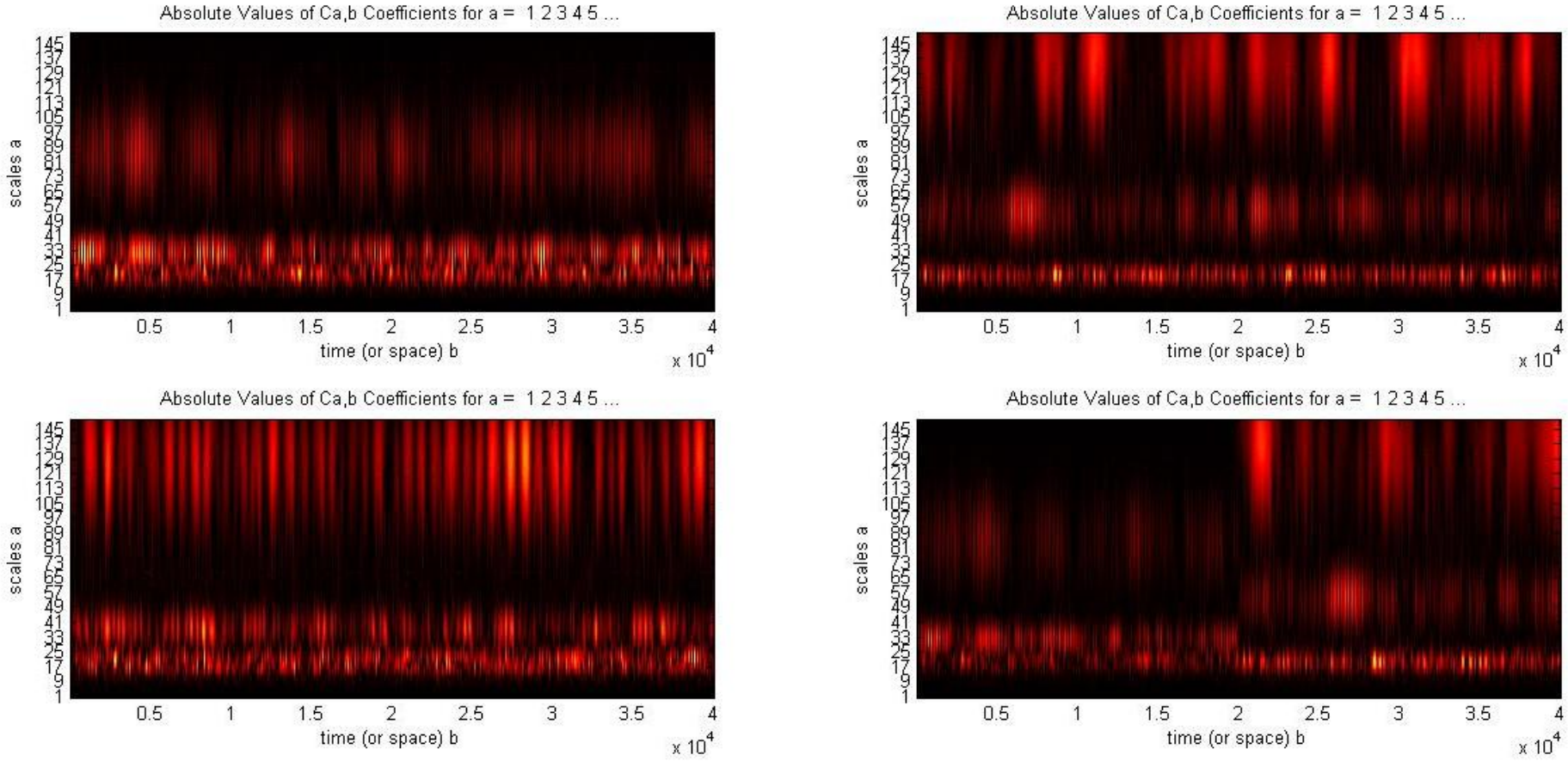

Fig. 4.6 Wavelet transform (2D) of the four cases (case1-case 4)

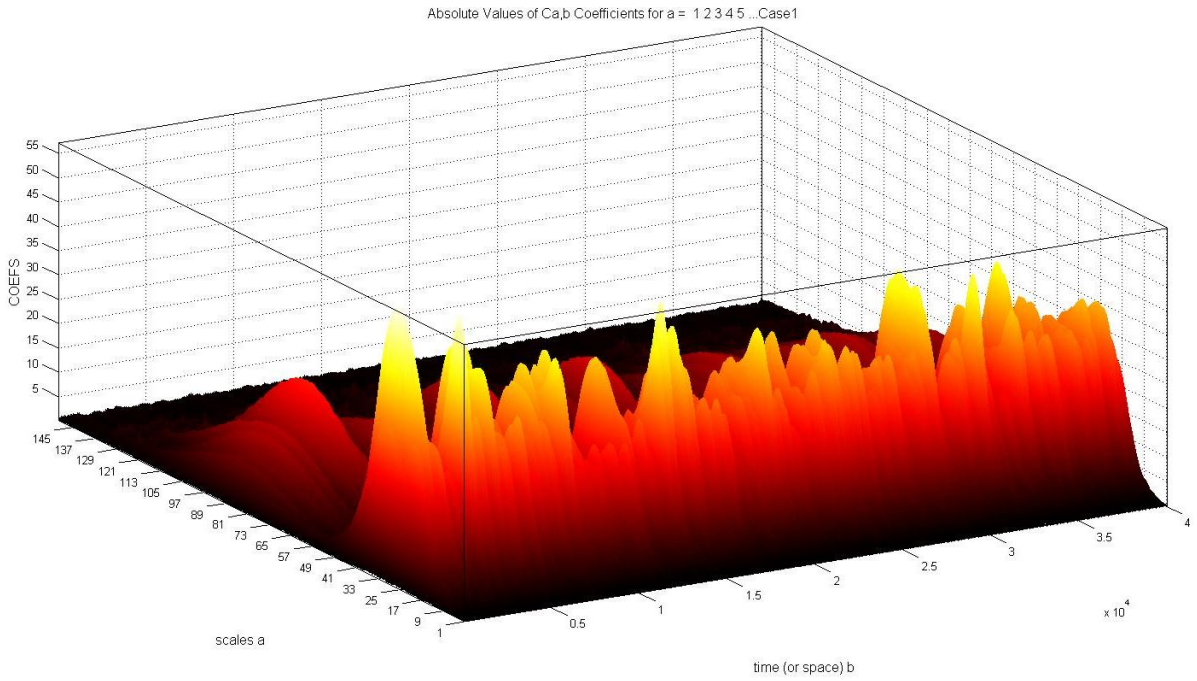

Fig. 4.7(a) 3D-wavelet transform for case-1

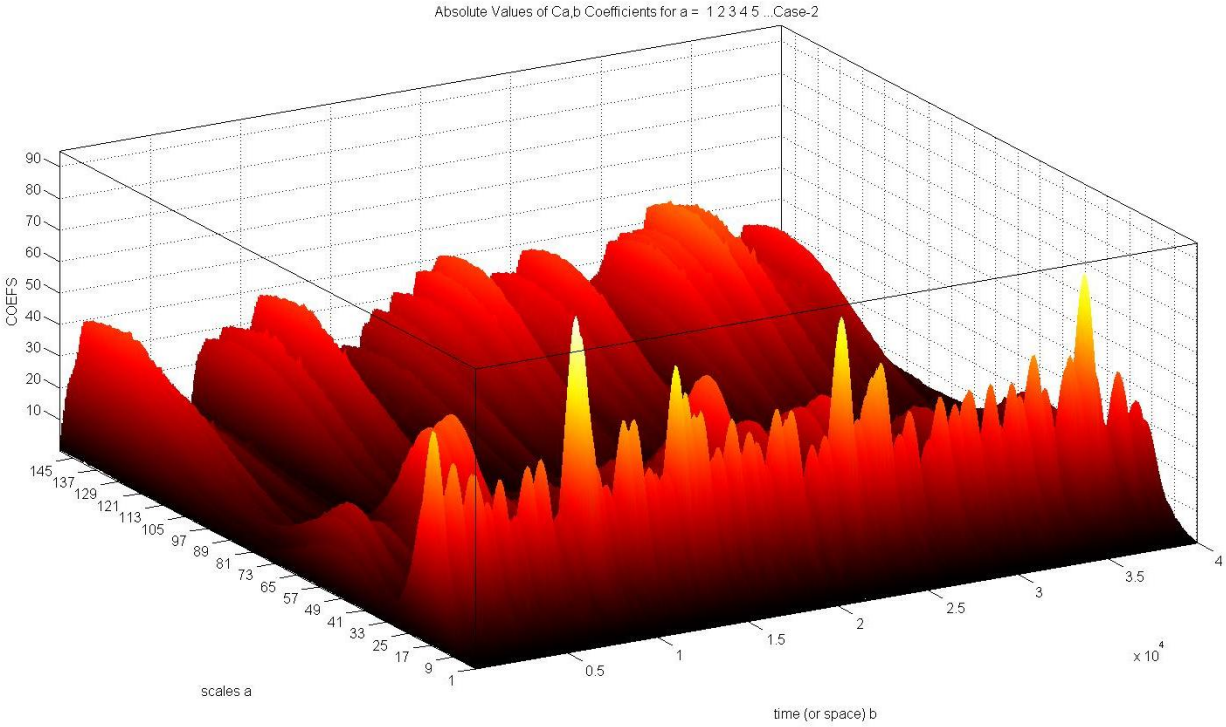

Fig. 4.7(b) 3D-wavelet transform for case-2

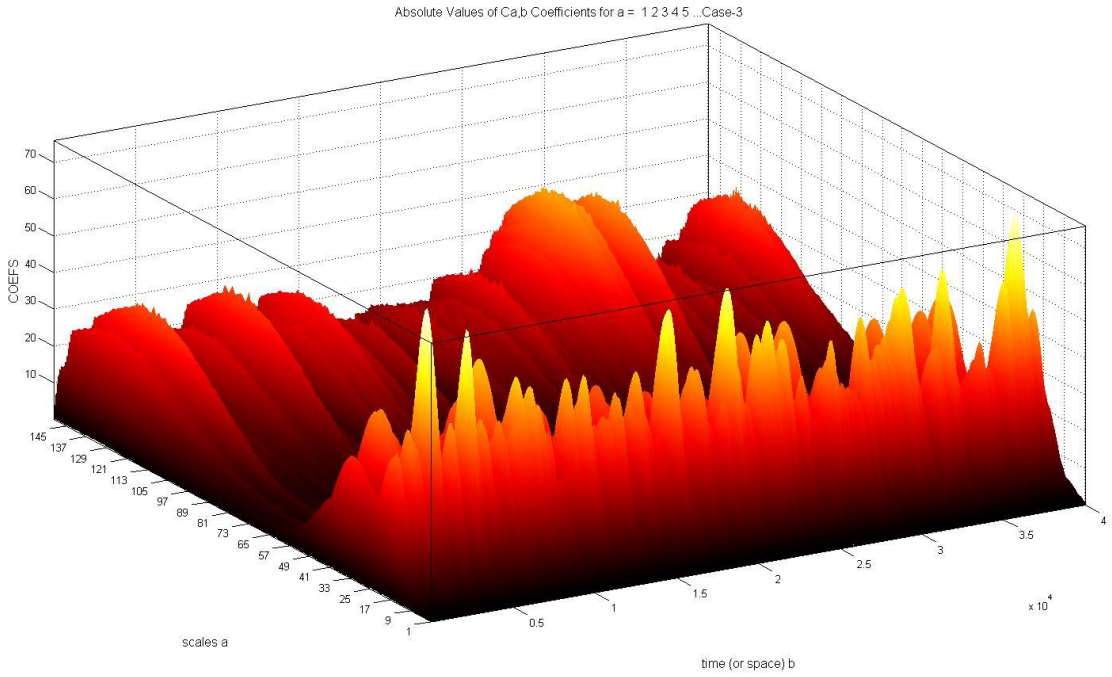

Fig. 4.7(c) 3D-wavelet transform for case-3

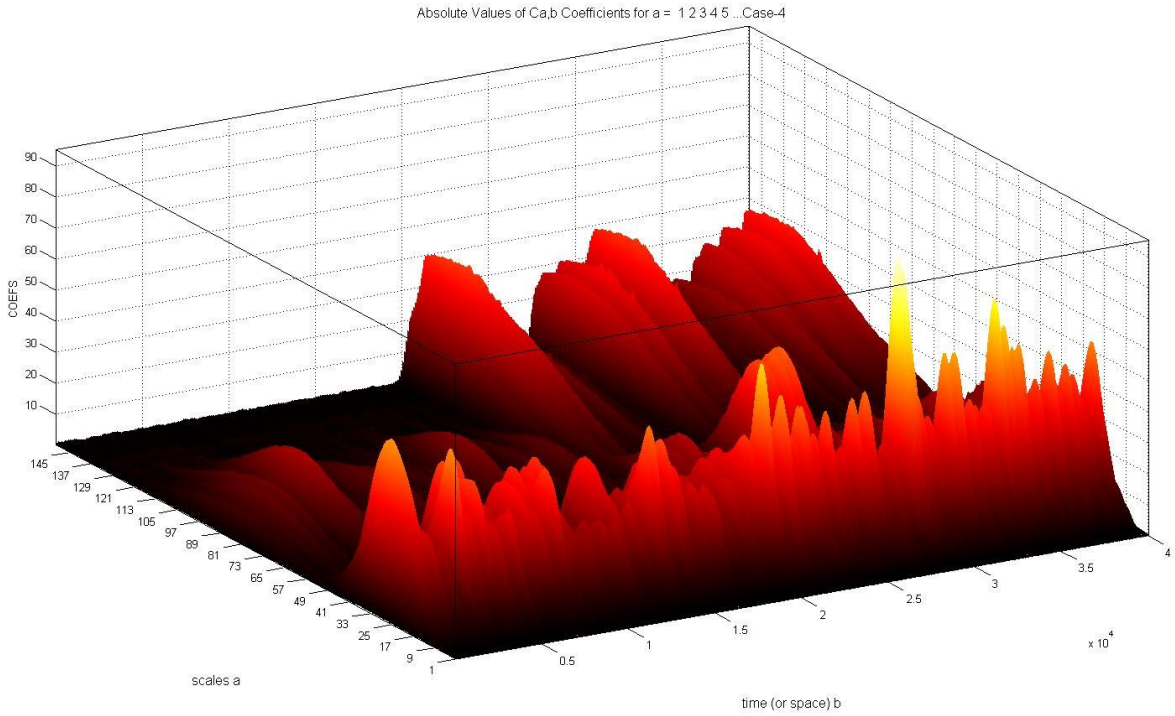

Fig. 4.7(d) 3D-wavelet transform for case-4

4.2.1 Fourier Transform of Simulation Data

From the Fourier transform in Fig. 4.5 each of the different cases seem to have 4-frequency mode components except for case-4. Table 4.3 shows the magnitudes of the four frequency modes obtained from each case. From the numbers one can understand or observe that the frequency obtained from the damaged data sources is less than data simulated from the undamaged. The amount of reduction varies for the different damage cases. For example each of the four frequency values for case-2 are less than case-3 implying that data induced from damage scenario case -2 is more severe that of case-3. Case-4 has more frequency mode components but the dominant values are as shown in Table 4.3.

Table 4.3 Fourier transform output values for the four damage cases

	Case 1	Case 2	Case 3	Case 4
Frequency mode 1	8.565	4.66	5.02	4.64
Frequency mode 2	20.24	11.97	17.18	11.83
Frequency mode 3	30.77	28.93	29.86	31.34
Frequency mode 4	38.32	32.06	38.32	33.26

Fig. 4.8 presents a summary of the frequency comparison of the four damage scenarios considered for the case study. From the figure it is apparent and imperative to expect that the frequency extracted from the undamaged case is higher compared with those from the damaged status. It also shows that the frequency gets even lower and lower as more severe damage is introduced to the structure.

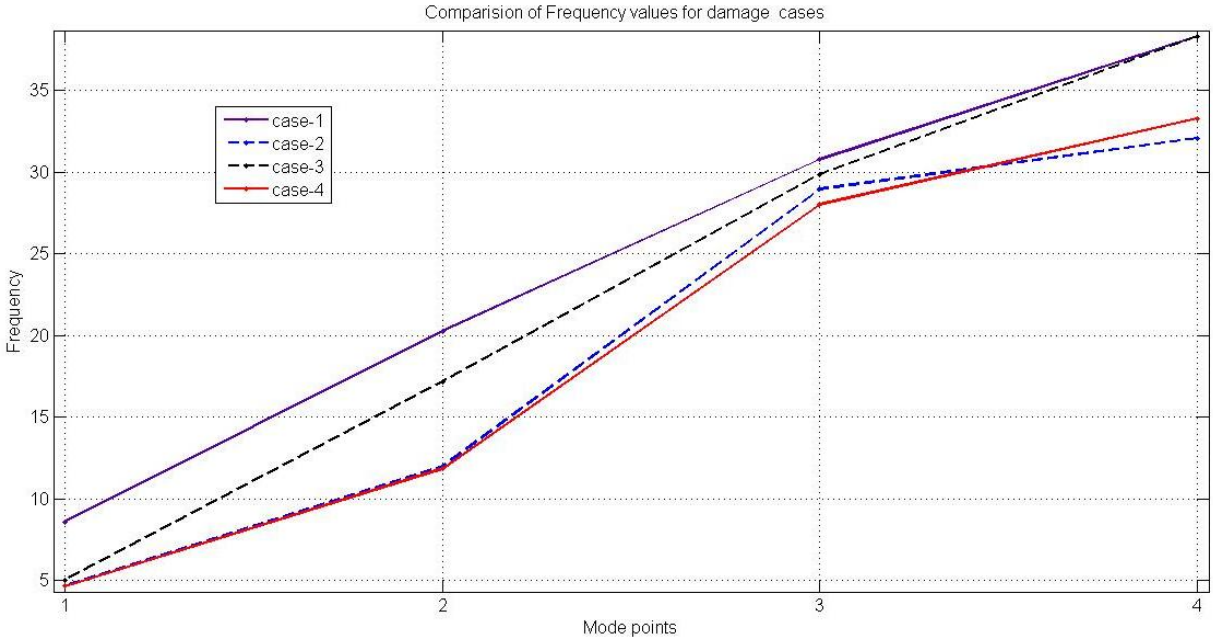

Fig. 4.8 Comparison of frequency from Fourier transform for the four damage cases

4.2.2 Wavelet Analysis of Simulation Data

From the scalogram plots of the four different damage cases shown in Fig. 4.6 and Fig. 4.7 one can compare and contrast the scale-translation representation both in 2D and 3D. The 2D plot shows only two axes: scale and time. The coefficients for each scale and combination are represented as color intensity. The 3D plots shown in Fig 4.7(a) - Fig 4.7(d) shows the wavelet transform in scale, time and coefficient axes unlike the 2D plots where the coefficients are represented in terms of color intensity.

In wavelet analysis a higher scale means lower frequency and vice versa. From wavelet transform of damage case-2 as shown in Fig.4.7(b) the peaks starting from around a scale of 81 to higher scale shows that the frequency has decreased and also the coefficient of lower scale values(higher frequency components)has decreased. While in

damage case-4 the scale starts to increase after around 20 sec which indicate that damage was introduced after 20 sec which is consistent with the simulation data. For the first 20 sec the plots for case-1 and case-4 looks almost the same as in Fig 4.7(a) and Fig 4.7(d).

By computing the coefficients at each scale of the simulation data, we can compare the plots both in 2D and 3D and observe the changes in the scale which indirectly represents frequency. One advantage that is gained by using wavelet analysis for this case study time information is available unlike the Fourier transform. In damage case 4 which is a combination of undamaged and damaged simulation data, it can be seen that around the 20 sec, the scale starts to increase indicating a frequency decrement and hence damage introduction to the structure.

4.2.3 Hilbert-Huang Application to Simulation Data

The four cases introduced in Table 4.2 were also considered to show the validity of the Hilbert Huang transform. Empirical Mode Decomposition (EMD) is applied to the different cases prior to Hilbert-transform and instantaneous frequency computation for each of the four cases. Fig 4.11 shows the Intrinsic Mode functions (IMFs) for case-1.

From the computation of EMD it is found out that the signal from the undamaged case has 11 IMFs. The Hilbert transform is computed for the first and second IMFs to obtain the phase diagram. From the phase diagram phase angle is computed. By differentiating the phase angle we can finally compute the instantaneous frequency which is the feature extraction or damage indicator which we are looking for. Recall the relationship between phase diagram, phase angle and instantaneous frequency from

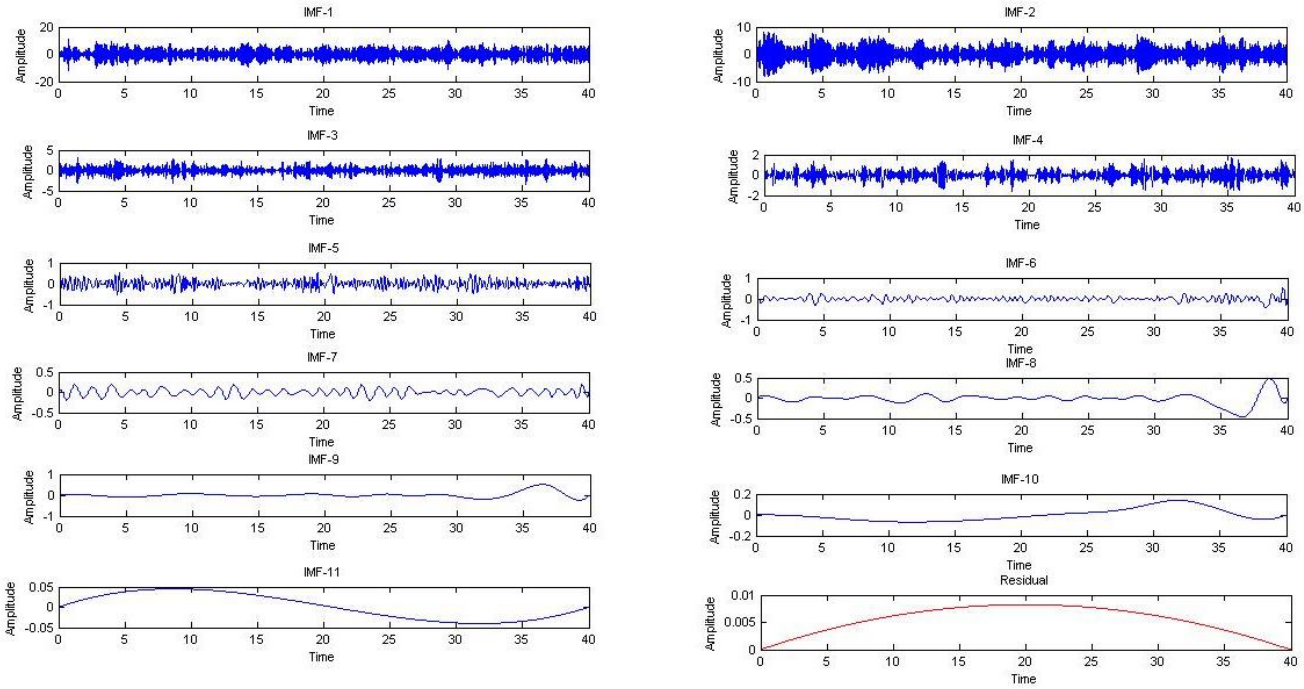

Fig. 4.9 IMF components of case-1 after EMD of the acceleration signal

section 3.2.3 of chapter 3.The same procedure is followed for the rest of the damage cases and the instantaneous frequency is extracted and the final output is as shown in Fig 4.10. The steps followed for the Hilbert transform can be revised in the following steps,

i. Sifting of a signal in to IMFs by using EMD

ii. Hilbert transform and Instantaneous frequency computation for IMFs.

From the instantaneous frequency plots (cases 1-4) from Fig. 4.10 it is difficult to see the difference in magnitude of frequency plotted for the damaged and undamaged cases. To be able to decide there is a difference in mean and variance from the cases considered, a statistical hypothesis test was conducted.

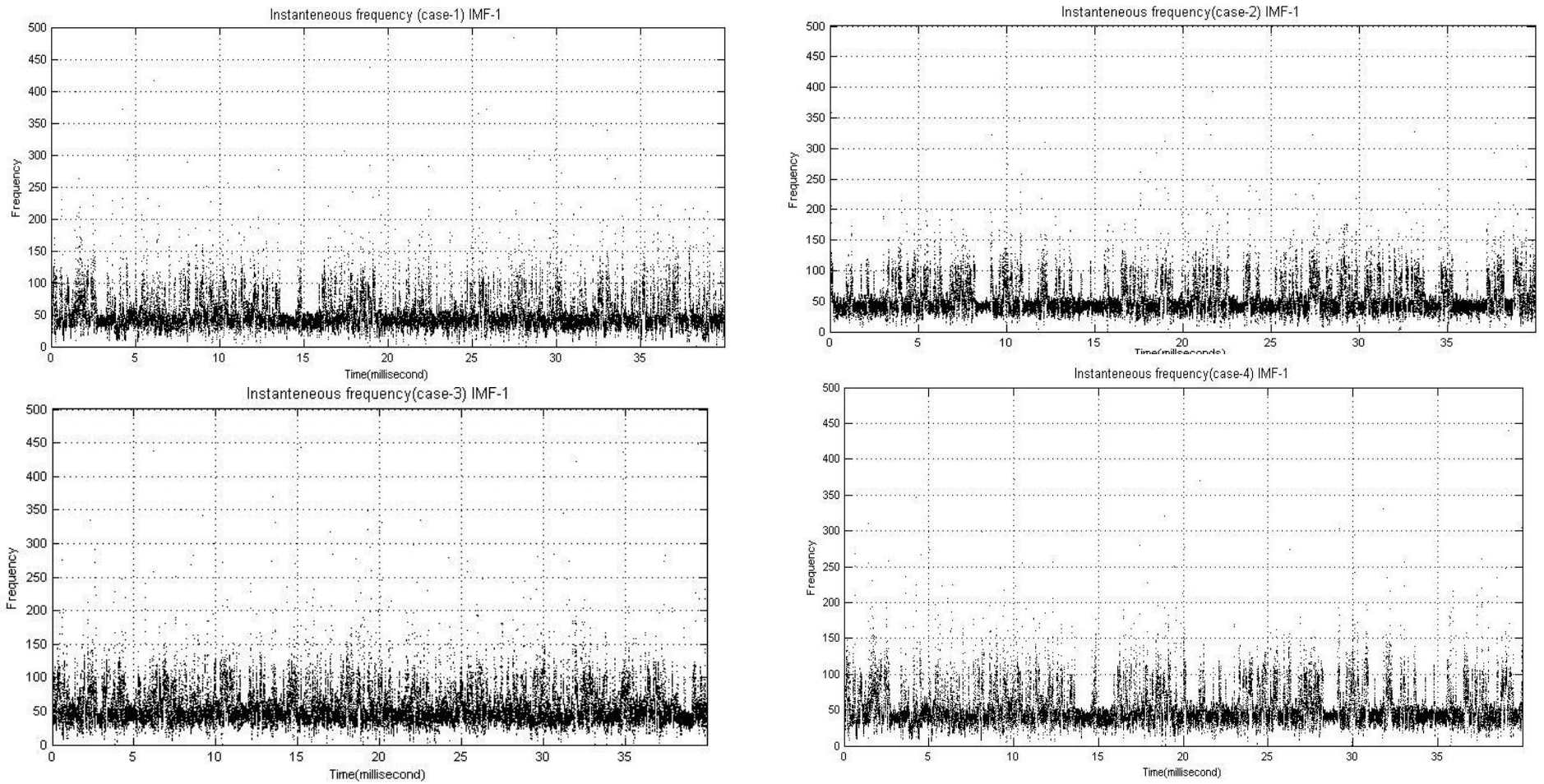

Fig. 4.10 Instantaneous frequency plot for (case-1-case-4) from the 1st IMF of each case

Statistical Hypothesis testing

In statistics hypothesis testing is done to draw inferences about a population based on statistical evidence from a sample. The instantaneous frequency values from the samples that were taken in the damaged (cases 2, 3, and 4) and undamaged condition (case-1) from the plots could not tell us if there is shift in mean and variance when damaged is introduced. Since the data being investigated are generated from two separate and independent groups (damaged and undamaged), the two tailed T-test for mean change and variance change was selected for the test.

Hypothesis testing for Mean change in the instantaneous frequency:

Null Hypothesis

- H_0: mu_1-mu_2=0 or (mu_1=mu_2) with unknown variance
- No mean change in the instantaneous frequency

Alternate Hypothesis

- H_1: mu_1-$mu_2 \neq 0$ or($mu_1 \neq mu_2$)
- There is change in the mean of the instantaneous frequency

where mu_1 and mu_2 represents the mean values from different and independent cases.

From Matlab statistical tool box the function h = ttest2(x, y) was selected to perform a *t*-test of the null hypothesis. The t-test assumes that x and y (the cases to be compared) are independent random samples from normal distributions. The result of the test is returned in h. h=1 indicates a rejection of the null hypothesis at the 10% significance level. h = 0 indicates a failure to reject the null hypothesis at the 10% significance level.

Hypothesis testing for variance change in the instantaneous frequency:

Null Hypothesis

- H_0: $s^2_1-s^2_2 = 0$ or $(s^2_1 = s^2_2)$
- No change in the variances of the frequency from two different cases

Alternate Hypothesis

- H_1: $s^2_1-s^2_2 \neq 0$ or $(s^2_1 \neq s^2_2)$
- There is change in the variances of the instantaneous frequency

where $\sigma^2_1$and σ^2_2 represents the sample variances from two independent set of data (frequency) to be compared.

From Matlab statistical tool box the function h = vartest2 (x,y) was selected to performs a *t*-test of the null hypothesis that the variances from two independent samples are the same. The result of this test is returned in h. h = 1 signifies a rejection of the null hypothesis at the 10% significance level where as h = 0 indicates a failure to reject the null hypothesis at the 10% significance level.

A Matlab algorithm was developed to do the hypothesis testing with a significance level of (α=0.1) that tests the null hypothesis every 1 sec for the whole time span of the sample data series which is 40 sec. Note that since the main focus here is to compare sample frequency changes in(mean and variance) from two different scenarios one damaged and the other undamaged and as a result, each of the three damaged conditions (case 2, 3, and 4) will be compared with the undamaged state (case-1).

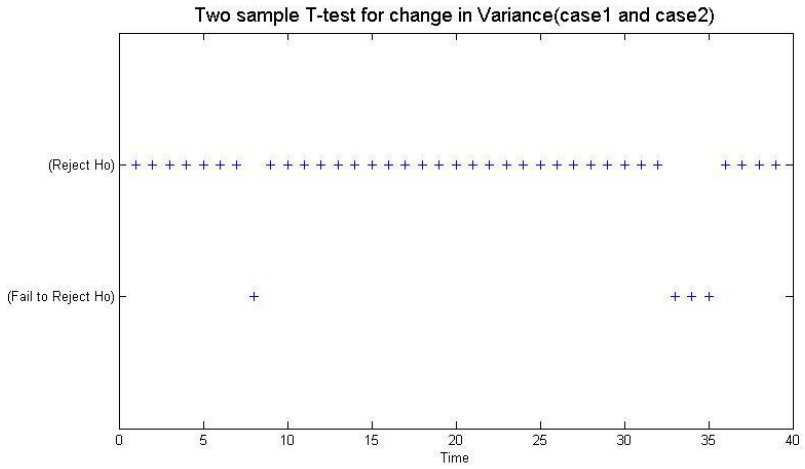

Fig. 4.11 Two sample (case1&case2) Variance test

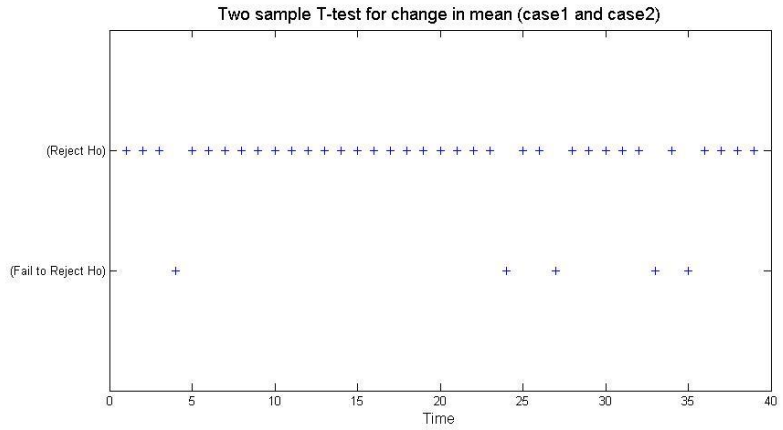

Fig. 4.12 Two sample (case1&case2) Mean test

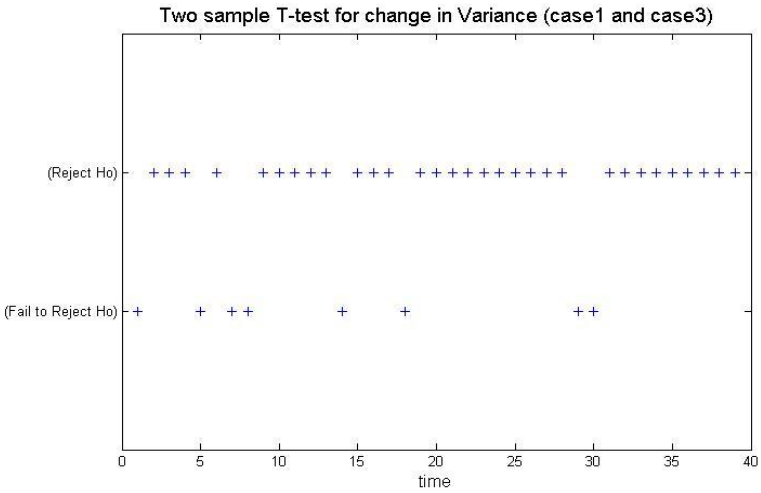

Fig. 4.13 Two sample (case1&case3) Variance test

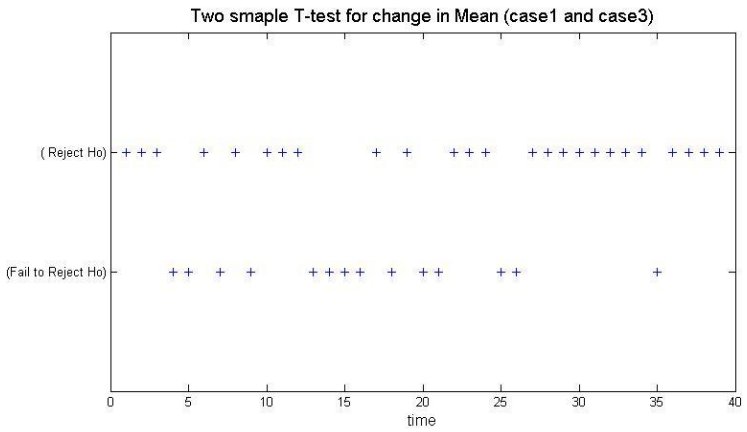

Fig. 4.14 Two sample (case1&case3) Mean test

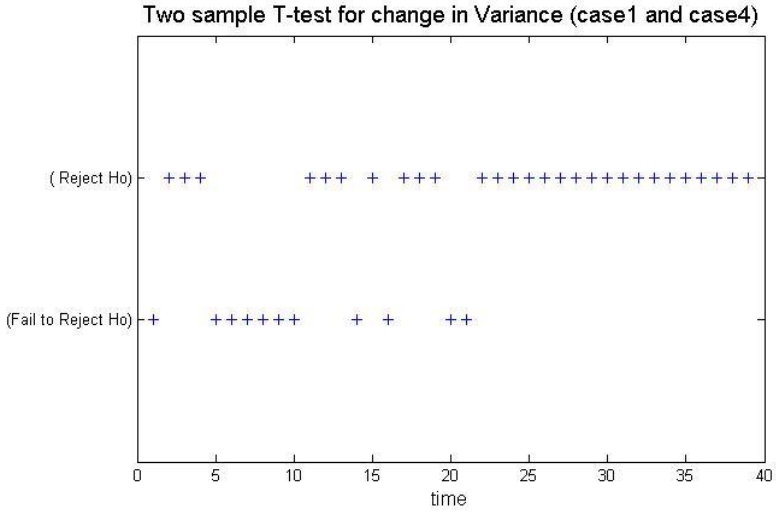

Fig. 4.15 Two sample (case1&case4) Variance test

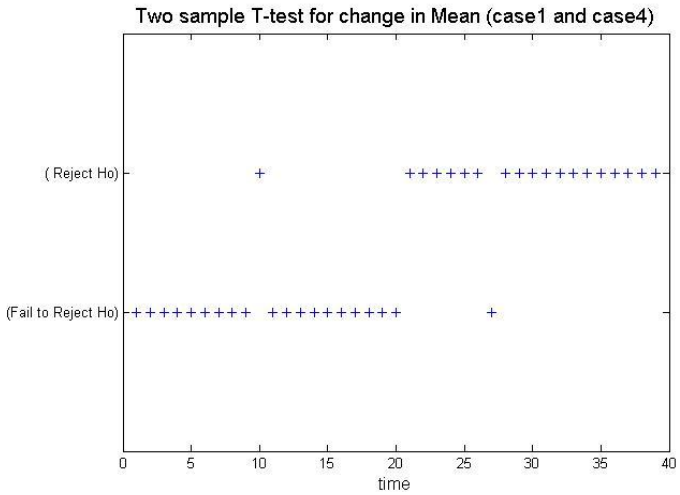

Fig. 4.16 Two sample (case1&case4) Mean test

From the hypothesis test results of change in mean and variance between case1 (undamaged) and the rest of the three cases (damaged), it is found out that the null hypothesis is rejected successfully as summarized in Table 4.4. The rejection of the null hypothesis implies that there is a difference in mean and variance from the two cases under study. For example the 90% rejection rate in variance test (case1 &case2) illustrates the frequency obtained from the two cases are different which is normal to expect since one is coming from a damaged and the other form undamaged case.

Table 4.4 Success rate of the mean and variance test in rejecting the null hypothesis

	Case1&Case2	Case1&case 3	Case1&case4
Variance test	90%	80%	95%
Mean test	87%	65%	95%

The higher successful rejection rate of case 2 compared with case3 shows that the proposed methodology is more sensitive and effective in differentiating between two cases as severe damage is introduced. Moreover it can be observed that the Variance test which measures the hypothesis, if two different distributions obtained from damaged and undamaged have the same variance or not, is shown to be more effective in successfully rejecting compared with the mean test.

Table 4.5 summarizes the output of variance and mean test conducted for other IMFs. From the table it can be observed that the successful rejection rate both by the

mean and variance of the hypothesis testing tends to increase when the comparison of instantaneous frequency is made for the 2nd, 3rd and 4th IMF values.

Table 4.5 Success rate of the mean and variance test in rejecting the null hypothesis from IMF-1 to IMF-4

	Case1 & Case2		Case1 & Case3		Case1 & Case4	
	Mean test	Variance test	Mean test	Variance test	Mean test	Variance test
1st IMF	87%	90%	65%	80%	95%	95%
2nd IMF	85%	92.5%	85%	87.5%	90%	65%
3rd IMF	95%	95%	92.5%	98.5%	90%	85%
4th IMF	97.5%	100%	97.5%	92.5%	95%	95%

A new case study (case-5) is created to show the efficiency of the proposed methodology of combining Hilbert transform and hypothesis testing to detect the progress from less severe to more severe damage. This case study is a combination of simulated data which comes from undamaged state, damage pattern-5, damage pattern-2 and damage pattern-1 which is described in Table 4.1. Note that the severity of damage increases one move from the 1-10 sec interval to the 31-40 sec interval.

Table 4.6 Damage patterns for case-5

Time period(sec)	Damage pattern
1-10	Undamaged(No braces removed)
11-20	(pattern-5).Removing one brace from the 1st and 3rd floor plus one of the beams partially unscrewed from the column
21-30	(pattern-1).Removing all braces in the 1st floor
31-40	(pattern-2).Removing all braces in the 1st and 3rd floor

The instantaneous frequency obtained from case-5 is compared with case-1 (obtained from data from undamaged situation) to observe the change in mean and variance between the two cases.

The result of the hypothesis test shows the change in the mean from the comparison of case-5 and case-1 is observable with time. The significance level for the hypothesis test is taken as (α=0.1). If the p-value of the test is less than 0.1 the null hypothesis is rejected and this rejection is line is represented by the dotted line as in Fig .4.17. From Fig.4.17 the majority null hypothesis (60%) is not rejected which shows that the data from for the first 10 sec is from undamaged since it is compared with case 1. For the time interval between 11-20 sec there is 80% rejection rate of the null hypothesis which indicates the mean of frequency has changed as a result of damage introduction. The 21-30 sec interval indicates a 90% rejection rate as data is coming from a more severe damage situation. Finally the 100% rejection rate of the null hypothesis indicates that the mean of the frequency from the cases of damaged and undamaged scenarios for the interval 31-40 sec are different. It is observed that the level of rejection of the null hypothesis varies for instantaneous frequencies obtained from different

From the application of Hilbert transform and hypothesis testing to the simulation data, change in the mean and variance (dispersion) of instantaneous frequency can be detected in with the inclusion of time information

By observing the mean and variance test plots from two different and independent instantaneous frequency plots, we can indicate at what time the difference in frequency occurs. Compared with the Fourier transform and wavelet analysis, the Hilbert transform together with the statistical hypothesis testing gives more information by quantifying the

damage level by indicating the successful rejection rate of the observed change in mean and variance of the instantaneous frequency.

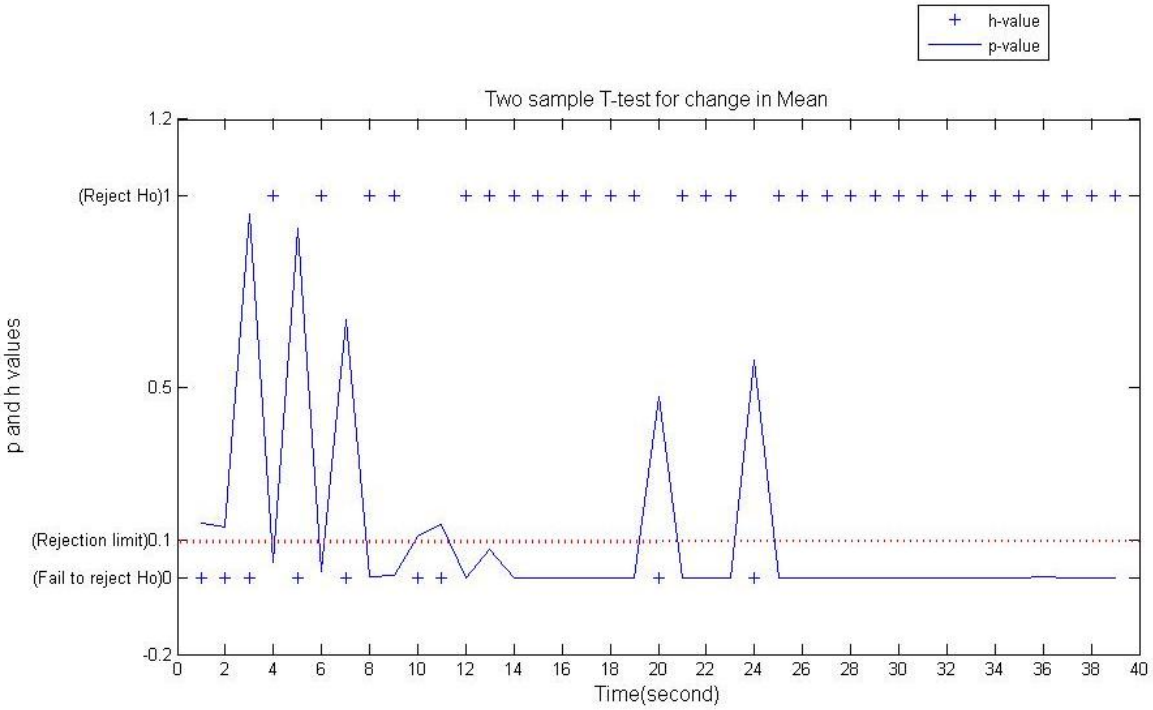

Fig. 4.17 Two sample mean test (case-1&case-5)

4.3 Statistical Analysis of Bridge Data

In this section measurements from different sensors are investigated using statistical tools to understand underling trends on the measured strain and temperature. Besides, the relationship between temperature and strain recordings is examined. The terminologies clomn-1 and column-2 are used throughout this section to differentiate between the two columns of the bridge.

To investigate the similarities and differences among the 4-sensors of column-1 a time series is plotted as shown in (Fig.4.19). From the plot it can be clearly seen that the

magnitude of deformation values for the 4-senosr varies with sensor 4 being with the highest magnitude of deformation followed by sensor-1, sensor-3 and sensor-2 respectively in descending order. The deformation recordings from sensor 4 are approximately 6 times larger than that of sensor-2.The same kind of deformation recordings variation is observed for column-2.

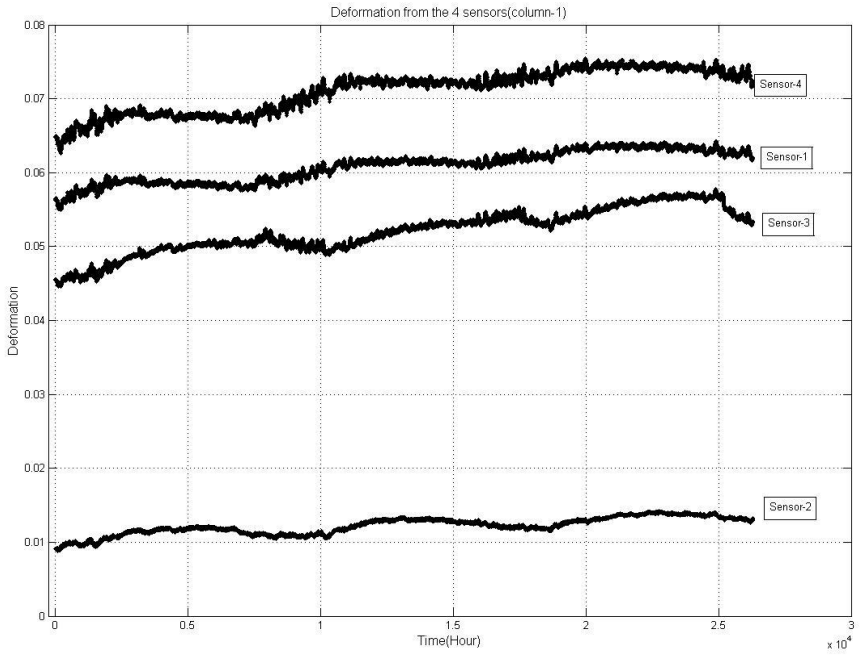

Fig. 4.18 Comparison of strain measurement from the 4 sensors of column-1

The correlation matrix given in Table 4.7 shows there is a significant relationship between the measured strain values of the four sensors. The correlation coefficient shown in the matrix is a single number which lies between -1 and +1 and it shows how strong the relationship between two variables is. A correlation coefficient (r) close to +1 shows a strong relationship between the two variables. Assuming we have two variables X and Y, the strength of the correlation coefficient r, is as interpreted in Table 4.8. The matrix plot

in Fig. 4.19 also proves the fact that the sensor strain recordings are correlated which is shown in terms of lines. The more the straight the line, the higher the correlation.

Table 4.7 Correlation coefficient among the 4-sensors

	Column-1(correlation)			
	sensor-1	sensor-2	sensor-3	sensor-4
sensor-1	1.00000			
sensor-2	0.86184	1.00000		
sensor-3	0.90971	0.90205	1.00000	
sensor-4	0.99155	0.84125	0.89387	1.00000

Table 4.8 Summary of correlation coefficient values

Correlation coefficient	Interpretation
r = + 1.0	As X goes up, Y always also goes up
r = + 0.5	As X goes up, Y tends to usually also go up
r = 0	No correlation
r = - 0.5	As X goes up, Y tends to usually go down
r = - 1.0	As X goes up, Y always goes down

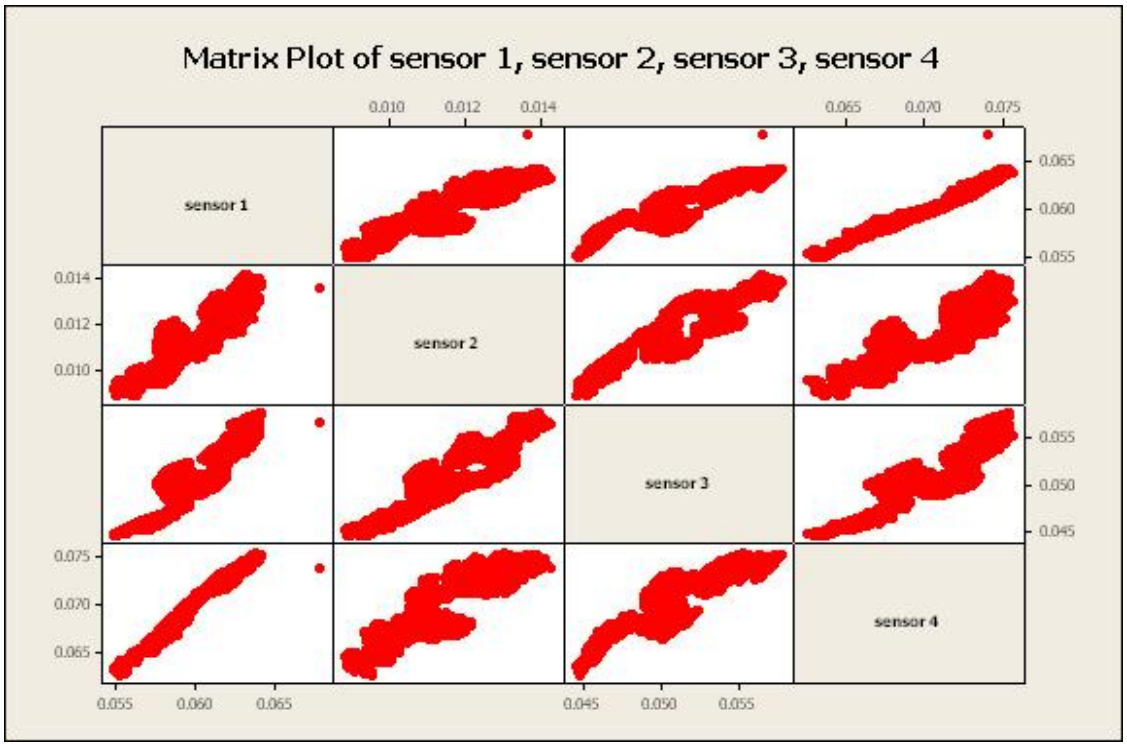

Fig. 4.19 Matrix plot showing the correlation among the 4-sensors

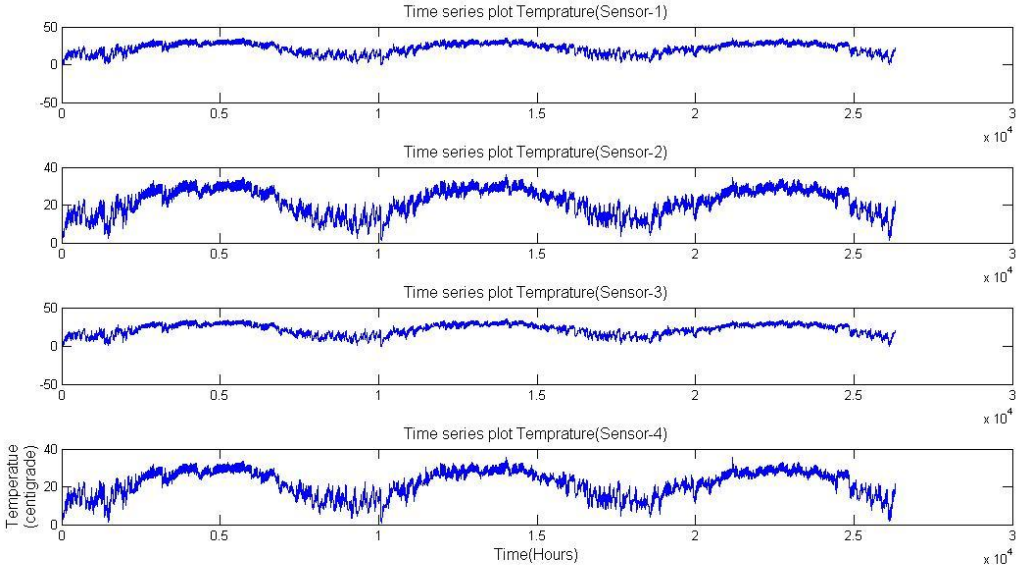

Fig. 4.20 Time series plot for the temperature readings at the 4-sensors from Column-1

From the plot of the temperature at each sensor of column-1, there is not only seasonality but also a very high amount of correlation between the sensor measurements. Seasonality is the periodic variation of a measured value over time. The temperature recordings are higher during the summer time and lower in the winter season. The correlation between the temperature measurements range between coefficient of correlation (r) value of 0.993 and 0.997.This implies that when the temperature measured at one sensor decreases (increase) so do the rest of the other sensor measurement values.

Relationship between sensor deformation measurement and temperature:

To study the relationship between temperature and strain readings, one sensor was selected. In Fig. 4.21, the standardized time series plot of deformation data for three years (2002-2004) and temperature measurement at the sensor location is illustrated. From the plot it can be clearly seen that there is seasonality with the temperature recordings where as for the strain data seasonality is observed after the data is de-trended. In time series analysis detrending is removing the slowly increasing or decreasing values or trend from a sequence of measured variables. The correlation coefficient between temperature and strain, r, is found to be around 0.275 before detrending of the strain data. After detrending of the sensor data the correlation between temperature and strain is found to be improved to r = 0.5218.

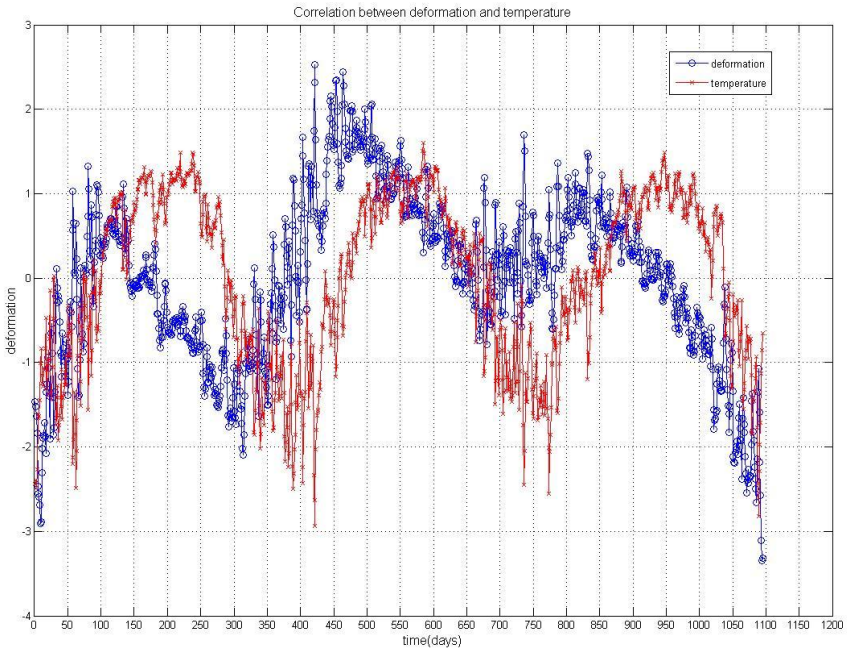

Fig. 4.21 Relationship between temperature and deformation recordings

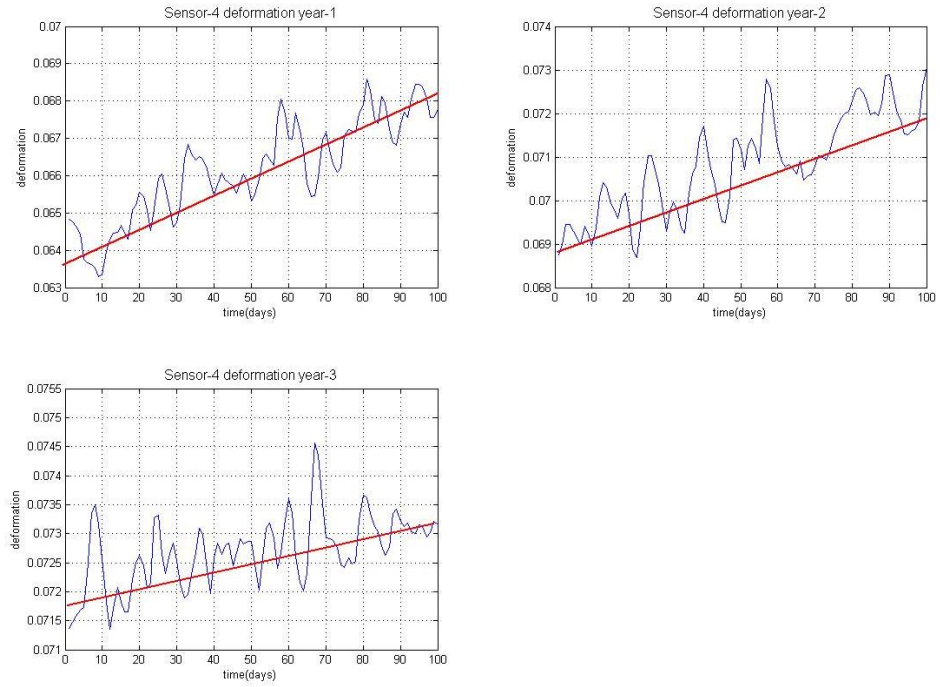

Fig. 4.22 Rate of increment of deformation for year 1, year 2 and year 3(sensor-4)

Table 4.9 Rate of increase of deformation for 4 sensors from column -1

	Sensor-1	Sensor-2	Sensor-3	Sensor-4
Year 1	$2.62*10^{-5}$	$1.74*10^{-5}$	$2.40*10^{-5}$	$4.02*10^{-5}$
Year 2	$1.81*10^{-5}$	$1.42*10^{-5}$	$2.82*10^{-5}$	$3.28*10^{-5}$
Year 3	$1.18*10^{-5}$	$1.21*10^{-5}$	$2.37*10^{-5}$	$1.17*10^{-5}$

From the fitted trend lines shown in Fig. 4.22, it can be seen that the slope of the line decreases as we go from the first year to the second and from the second to the third year. This indicates that the rate of deformation decreases every year. Table 4.7 summarizes the rate of increment of deformation per day for all the 4-sensors.

From Table 4.9 generally it can be seen that the rate of deformation decreases as we go from the first to the third year for each of the sensors. There is always an increase in the recorded deformation from year to year with different magnitude for each sensor; the rate of increase of deformation for sensor-3 is the highest.

4.4 Time Series Modeling for Bridge Data

A time series plot was made as shown in Fig. 4.23for one of the sensors (sensor-4) for different time intervals: 3 months, 6 months, 1year and 3 years to observe how the deformation recordings behave for different time intervals.

From the time series plot of strain measurement data for all the different time periods taken, the data is non-stationary as the value strain is increasing throughout time (mean is changing). For time series modeling approaches to be applied, first we should make the linear data stationary. The following section shows the detailed analysis for time period selected for 3-years.

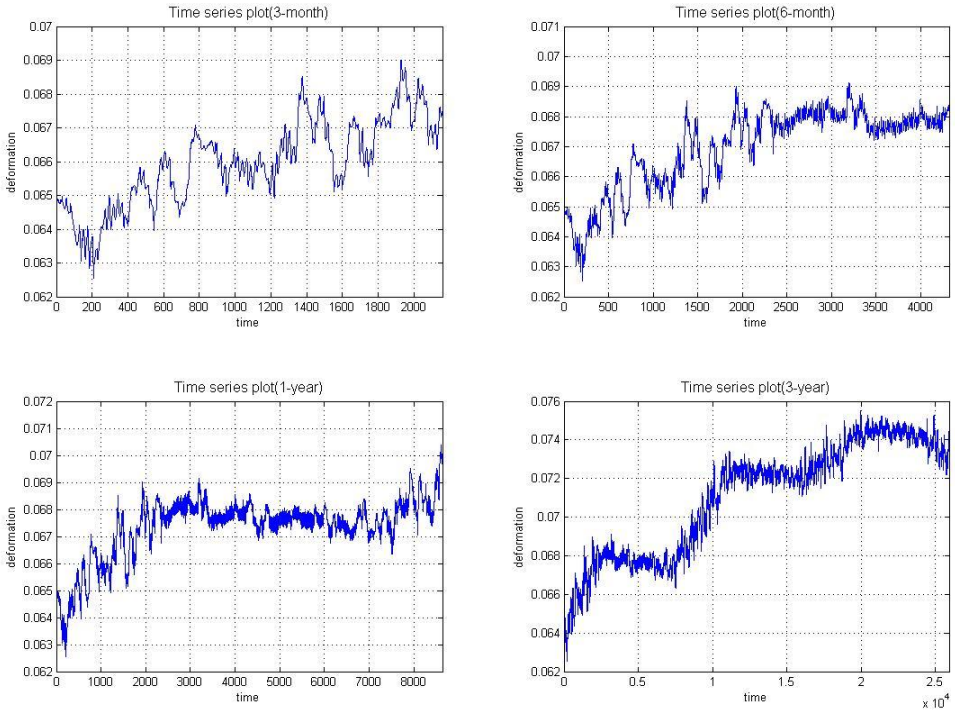

Fig. 4.23 Time series plot for sensor-4 with different time period

The time series analysis contains four main steps which are time series plotting, model identification, parameter estimation and diagnostic checking.

Step1: Time Series Plotting

From Fig. 4.24 since the data is non-stationary we should be able to find a way to make it stationary. Power transformations are applied to improve the interpretability of data or appearance of graphs. A Box- Cox test was employed to identify what kind of power transformation is appropriate to the data. Based on the test from Fig.4.25 the type of transformation that we should use is taking the square of the raw time series data. The 95% confidence interval for λ contains a value closer to 2, and this strongly suggests taking the squared value for the sensor data.

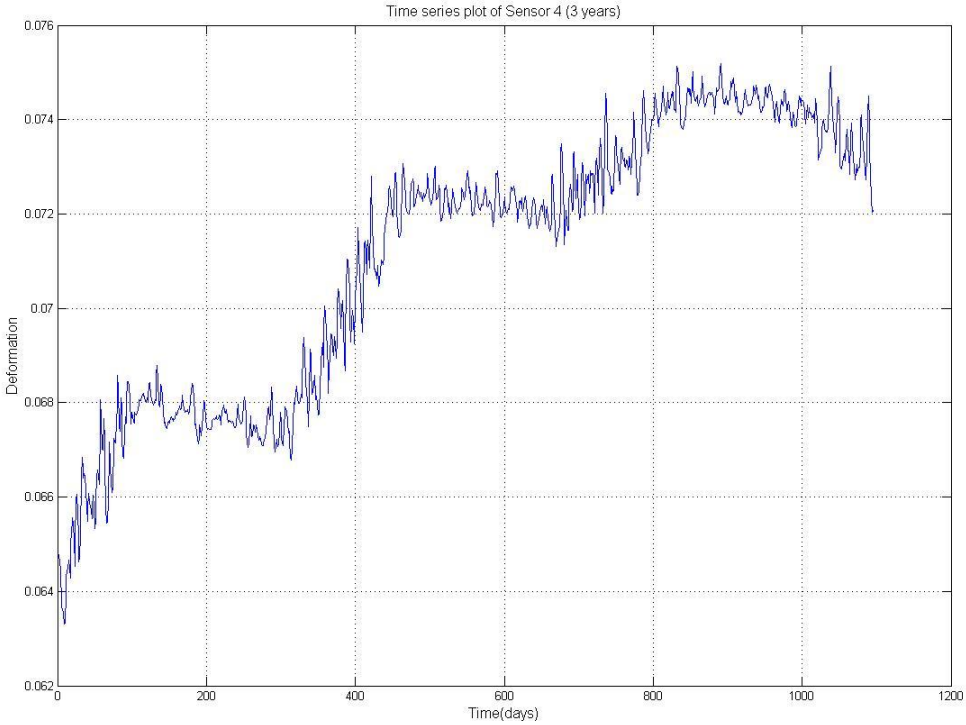

Fig. 4.24 Time series plot for sensor-4 (3-years)

Step2: Model Order Selection

Since the data is non-stationary we should take the first differencing as in Fig 4.25.To support the decision for taking the differencing, the augmented Dickey-Fuller (ADF) test statistic was performed. The null hypothesis test for ADF is that the data to be tested is non-stationary while the alternate hypothesis being data is stationary. By running this test for the squared sensor data at a significance level of α=0.1 it is found that the p value is 0.7905 which fails to reject the null hypothesis. This suggests the hypothesis that the data stationary holds valid.

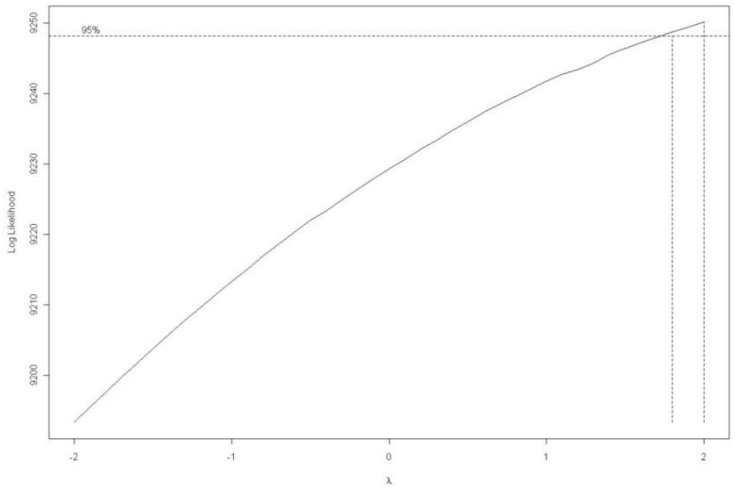

Fig. 4.25 Box-Cox plot for sensor-4

Assume that x(t) is data for sensor-4 taken for 3 years , from the Box-Cox test we knew that we have to take the square of the data, and let $y(t)=x(t)^2$. The expression diff(y(t)) indicates that a differencing is taken for the time series data y(t) and it can be defined by diff(y(t))= $\nabla y_{(t)}=y_{(t)}-y_{(t-1)}$. The plot for the diff(y(t)) is illustrated in Fig. 4.26.

The main task in this step is determining the order of the model by plotting the partial autocorrelation (PACF) and autocorrelation (ACF).

From Fig.4.27 the ACF plot seems tailing off slowly which makes it uncertain to determine the order for MA process (q). The PACF plot shows the values seem to cut off after lag p=2 but there is significant correlations between lags and 10. To determine the correct order for the model, the extended autocorrelation function (EACF) was performed to get the values shown on Table 4.10. From the EACF select a triangular region of 0 values (shown in Table 4.10) and start from the top left vertex which gives the least combination of AR and MA model parameters. From the possible combination of AR and MA orders, select orders with the least p and q value. From the possible combination the model orders (p,d,q) , (3,1,2) and (1,1,4) seems a valid model.

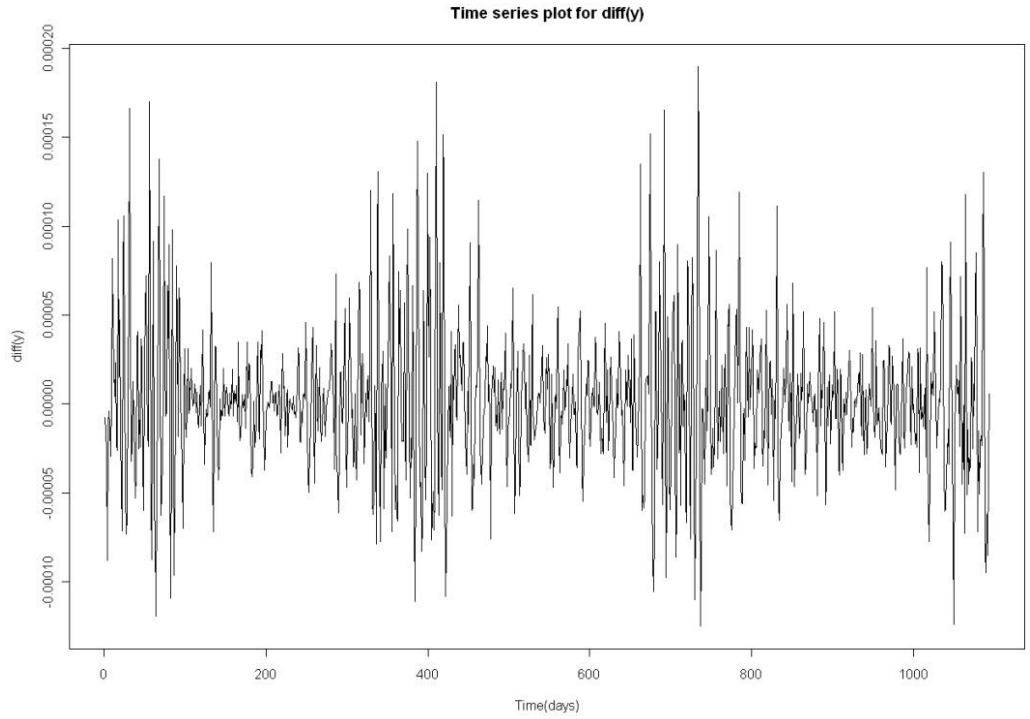

Fig. 4.26 Time series plot for diff(y(t))

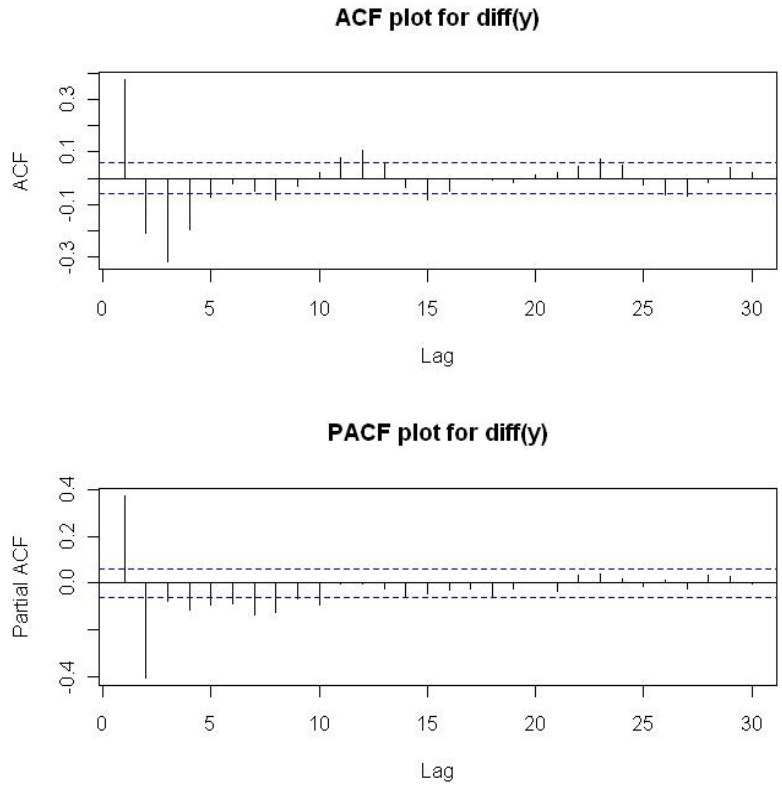

Fig. 4.27 ACF and PACF plot for diff(y(t))

Step 3: Parameter Estimation

Once we have identified the model orders the next step is estimation of the parameters. The R-statistical software output of the two model orders selected, i.e. c=(3, 1, 2) and c= (1, 1, 4) are as shown in Fig. 4.28.

Table 4.10 Sample extended autocorrelation function (EACF) for diff(y)

AR/MA	0	1	2	3	4	5	6	7	8	9	10	11	12	13
0	X	X	X	X	X	0	0	X	0	0	X	X	0	0
1	X	X	X	X	0	0	0	X	0	0	0	X	X	0
2	X	X	X	X	0	0	0	X	0	0	0	0	0	0
3	X	X	0	0	X	0	0	X	0	0	0	0	0	0
4	X	X	0	0	X	0	0	X	0	0	0	0	0	0
5	X	X	X	0	0	0	0	0	0	0	0	0	0	0
6	X	X	X	X	0	X	0	X	0	0	0	0	0	0
7	X	X	X	X	X	X	X	X	X	X	X	0	0	0
8	X	X	X	X	X	X	0	0	X	X	X	0	0	0

Call:

arima(x = y, order = c(3, 1, 2))

Coefficients:

ar1	ar2	ar3	ma1	ma2
1.0031	**-0.4295**	**0.0356**	**-0.5838**	**-0.2542**
s.e. 0.1368	0.1614	**0.0838**	0.1342	0.1110

sigma^2 estimated as 1.085e-09:

log likelihood = 9737.98,

aic = -19465.96

Call:

arima(x = y, order = c(1, 1, 4))

Coefficients:

ar1	ma1	ma2	ma3	ma4
0.3151	**0.1058**	**-0.3966**	**-0.3205**	**-0.1065**
s.e.0.0960	0.0960	0.0407	0.0464	0.0517

sigma^2 estimated as 1.089e-09:

log likelihood = 9736.37,

aic = -19462.75

Call:

arima(x = y, order = c(2, 1, 2))

Coefficients:

ar1	ar2	ma1	ma2
0.9485	**-0.3636**	**-0.5309**	**-0.2969**
s.e. 0.0464	0.0445	0.0470	0.0444

sigma^2 estimated as 1.086e-09:

log likelihood = 9737.9,

aic = -19467.81

Fig. 4.28 R-output for parameter estimation for model orders c=(3,1,2) c=(1,1,4) and c=(2,1,2)

From the order model c=(3,1,2) it can be seen that the coefficient for Ar-3 is not significant implying there Ar-3 is non-existent in the model and due to this reason, it is desired to fit a model of order C(2,1,2) whose parameters are estimated in Table 4.28(c). The coefficients for the order=c(1,1,4) are all significant and finally we need to compare model c=(2,1,2) and C(1,1,4) by comparing the AIC and log likelihood values. Based on the AIC and log likelihood values the best model for diff(y) would be ARIMA (2,1, 2). The model fitted can be written as in Eq.(4.1).

$$\nabla y^2_{(t)}=0.9485\nabla y^2_{(t-1)}+ 0.3636\nabla y^2_{(t-2)}- 0.5309\nabla w^2_{(t-1)}- 0.2969\nabla w^2_{(t-2)}+ w_{(t)} \quad 4.1$$

The fitted model ARIMA (2,1,2) is when three years of data is taken. The same procedure is followed to fit a time series model considering only a one year data and the model fitted is found to be ARIMA (0,1,2). This shows that the number of data points taken has a huge effect on the final model selection.

Step 4: Model Diagnostics

This step is used to examine the goodness of fit of the selected model. If the goodness of fit is poor, it is desired to redo the model fitting part again or time series model may not be fitted at all. The residual which is the difference between the actual and predicted model will be diagnosed to indirectly assess the validity of the selected model. A model selection is deemed good if the model residual properties are close to white noise.

From Fig. 4.29 the first plot that shows the standardized plot of the residuals suggest a rectangular scatter around zero with no trend. This suggests that the residuals are close to a white noise. The second plot indicates the autocorrelation of the residuals.

For a pure white noise these residuals should be uncorrelated and normally distributed with zero means and some variance. Based on the autocorrelation plot of the residuals it seems that it is uncorrelated which is a good indication that the selected model is appropriate. The third plot illustrates that the hypothesis test that the residuals are correlated is not rejected since the p-values are greater than the significance level. The normality plot Fig. 4.30 also shows that the residuals follow a normal distribution except for a slight distortion at the end points.

From the time series modeling for the bridge data it is noted that

(i) The model order selection is greatly affected by the number of data points. Two different types of models were found for the same set of data but different number of points. Taking 3 year data and 1 year data has resulted in model orders of c= (2,1,2) and (0,1,2) respectively.

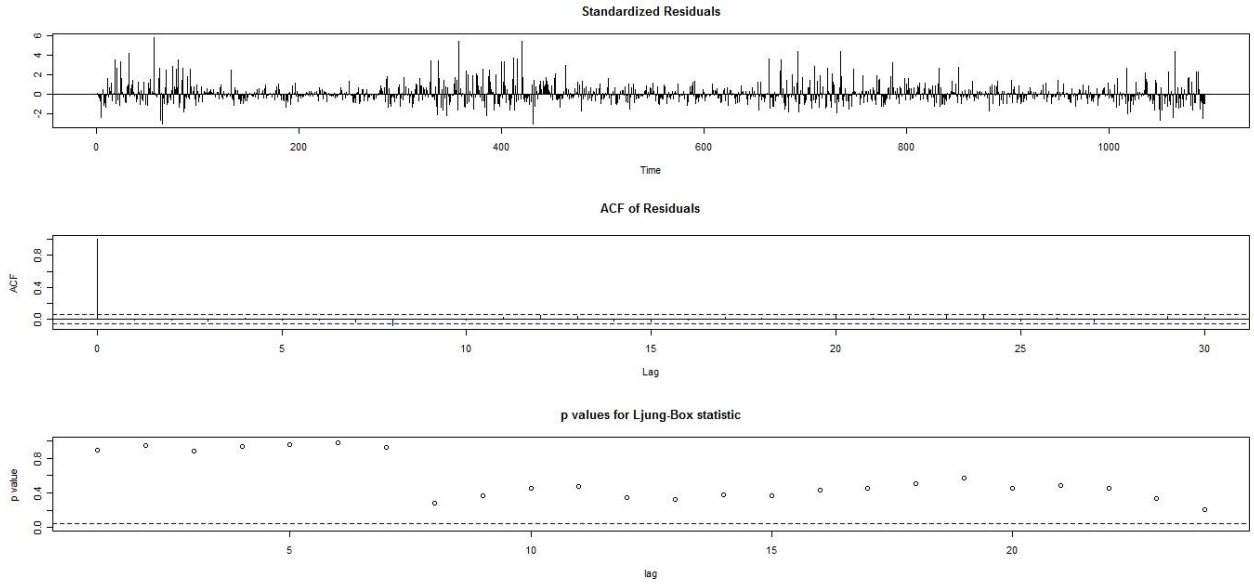

Fig. 4.29 Diagnostic plot for the fitted ARIMA c=(2,1,2) model

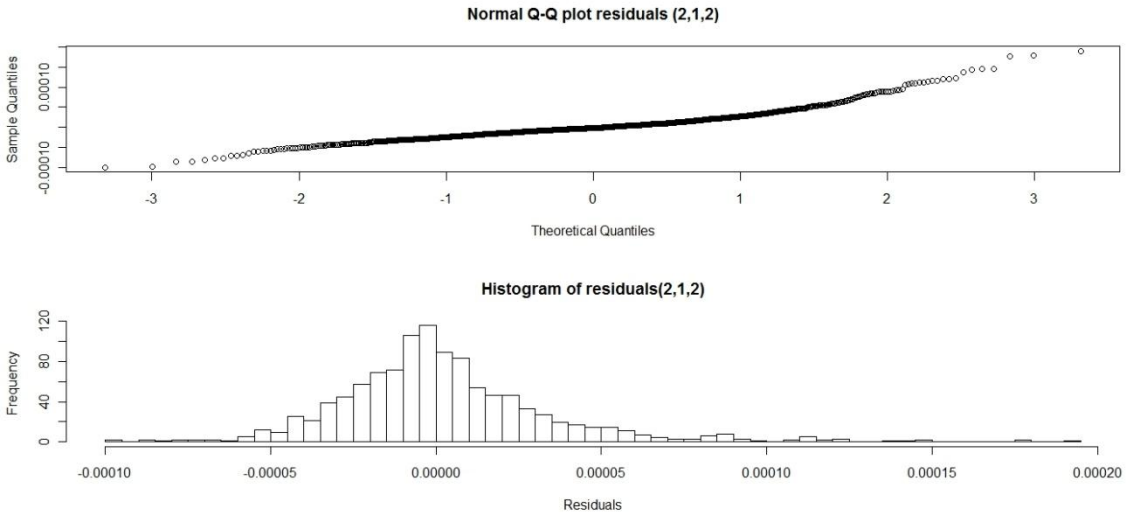

Fig. 4.30 Normality test for residuals

(ii) Based on the fitted model future recordings from the sensors can be compared with the coefficients of the ARIMA model. The change in the coefficients of the model will indicate the deviation from the base line of comparison. By monitoring this change in coefficients, data can be analyzed if it is from a normal or damaged state by comparing it from the undamaged state.

CHAPTER V

SUMMARY AND CONCLUSION

5.1 Summary of Findings

The proposed research was aimed at damage detection of civil structures bridges based on response data from sensors. The applied damage detection methodologies were time series modeling and frequency domain analysis. The validity of the approaches was shown through application of simulation data designed on a benchmark problem by the ASCE task group and data from a functional bridge. The case study of simulation data considered in this research is aimed to show the capability of the proposed approaches to determine the change in the frequency from different sources of simulated data.

According to the case studies conducted the frequency domain approaches were shown to be effective on identifying the presence of abnormality (change in frequency) from data captured from a damaged condition. In the study simulation data generated from three different damage cases and one normal condition were considered. Simulated data collected from the undamaged was taken as a baseline of comparison with the other set of data from a damaged state. According to Huang *et el*., 2005, when damage is introduced in to a system the dynamic behavior will change and this can be observed in

the modal parameters of the system such as frequency. Therefore, the main target in transforming the raw acceleration time series data in to Fourier, wavelet and Hilbert transform is to monitor the change in frequency from the data simulated from normal and abnormal conditions.

Fourier transform of data from a normal and damaged condition of the civil structure were compared and it is found out that the frequency obtained from a damaged case were less in magnitude compared with the normal state. Since Fourier analysis lacks time information we have no clue as to when the damage started to occur in the structure.

The wavelet analysis deals with the time information which is better than the Fourier analysis. Damage case-4 defined in Table 4.2 is a combination of undamaged data for the first 20 sec and damaged for the next 20 sec. The wavelet analysis applied to this specific case for detecting the damage progress showed in the scalogram representation that the scales of the transformed signal increases after 20 sec. This shows that the method is able to capture the change in frequency after damaged is introduced in the system.

EMD and Hilbert Transform for extraction of the instantaneous frequency (frequency dependent on time) coupled with hypothesis testing were applied to the simulation data. For the purpose of demonstration of the effectiveness of this approach only analysis based on the first IMFs are shown in this study. In general the hypothesis testing and Hilbert transform, detected the change in frequency of the cases in form of rejecting and failure to rejecting the change in mean and variance of instantaneous frequencies. From the two methods of hypothesis testing experimented, the change in variance of the frequencies is found to be more effective and sensitive to successfully

reject the null hypothesis defined as no change in mean and variance of instantaneous frequency. It is also observed that the Hilbert transform applied is dependent on the IMF applied to get the instantaneous frequency.

In this research the formal procedures in time series procedures were applied to data acquired from a functional bridge. It should be noted that the time series model fitting is dependent on the number of data points taken for the analysis. It is observed that taking different data sizes for the same sensor data will result in a different model order selection. Based on fitted ARIMA models future deformation recordings from the sensors can be forecasted which benefits in determining the extent of deformation and taking proactive measures.

The statistical analysis has shown that there exists a high correlation between the measured deformation values and different sensors. It is also shown that temperature and deformation have a high correlation. Seasonality in the temperature recordings was observed where as the deformation was observed to increase with time. From the analysis it is observed that the level of deformation increment is dissimilar for different sensors.

5.2 Future Work

There are several barriers to the widespread use of sensors in bridges. One significant problem is that there is scarcity of adequate data showing a failed bridge. Due to this problem data analysis for bridges is limited to laboratory or experimentally simulated data. The problem with using these kinds of data is that the actual operational and environmental conditions at which the bridge experiences cannot be simulated well. One reason to this problem is the capability of finite element simulation software since

environmental parameters such as temperature, wind; humidity etc. cannot be easily incorporated into the model.

Due to this problem more advanced data analysis methodologies such as time series analysis for non-stationary and non-linear data is the aim of future study. In this study a series of approaches such as power transformation and differentiation were applied to make the data stationary. It should be noted also that this process will conceal the inherent feature of the data which will lead to a different results and conclusion. The selection of optimal IMF for Hilbert transform and instantaneous frequency extraction is the subject of future study due to the different outputs obtained by applying selected IMFs.

REFERENCES

Problem Solving with Computers. from http://www.isr.umd.edu/~austin/ence200.d/software.html

AASHTO. (2007). *Bridge Design Specifications*. Washington, DC.

Bassiuny, A., Li, X., & Du, R. (2007). Fault diagnosis of stamping process based on empirical mode decomposition and learning vector quantization. *International Journal of Machine Tools and Manufacture, 47*(15), 2298-2306.

Bayissa, W., Haritos, N., & Thelandersson, S. (2008). Vibration-based structural damage identification using wavelet transform. *Mechanical Systems and Signal Processing, 22*(5), 1194-1215.

Box, G. E. P., Jenkins, G. M., and Reinsel, G. C. . (1994). *Time Series Analysis, Forecasting and Control,* (3rd ed.). Englewood Clifs, NJ. : Prentice Hall.

Carden, E., & Brownjohn,J. (2007). ARMA modelled time-series classification for structural health monitoring of civil infrastructure. *Mechanical Systems and Signal Processing, 22*, 295-314.

Chen, J., Xu, Y., & Zhang, R. (2004). Modal parameter identification of Tsing Ma suspension bridge under Typhoon Victor: EMD-HT method. *Journal of Wind Engineering and Industrial Aerodynamics, 92*(10), 805-827.

Doebling, W., & Farrar,C. . (1997). *Using Statistical Analysis to Enhance Modal-Based Damage Identification, in Structural Damage Assessment Using Advanced Signal Processing Procedures.* Paper presented at the Proceedings of DAMAS '97, University of Sheffield, UK.

Fugate, M., Sohn, H., & Farrar, C. (2001). Vibration-based damage detection using statistical process control. *Mechanical Systems and Signal Processing, 15*(4), 707-721.

Hou, Z., Noori, M., & Amand, R. (2000). Wavelet-based approach for structural damage detection. *Journal of Engineering Mechanics*, *126*(7), 677-683.

Huang, N., & Attoh-Okine, N. (2005). *The Hilbert-Huang transform in engineering*: CRC Press.

Huang, N., & Shen, S. (2005). *Hilbert-Huang transform and its applications*: World Scientific Pub Co Inc.

Johnson, E., Lam,H.,Katafygiotis,L.,& Beck,J. (2004). Phase I IASC-ASCE Structural Health Monitoring Benchmark Problem Using Simulated Data. *Engineering Mechanics*, *130*(1), 3–15.

Kullaa, J. (2003). Damage detection of the Z24 bridge using control charts. *Mechanical Systems and Signal Processing*, *17*(1), 163-170.

Lam, P. (2000). Matlab files for the Benchmark problem. from http://bc029049.cityu.edu.hk/asce.shm/phase1/asce_linkspage.asp

Li, H., Zhang, Y., & Zheng, H. (2009). Hilbert-Huang transform and marginal spectrum for detection and diagnosis of localized defects in roller bearings. *Journal of mechanical science and technology*, *23*(2), 291-301.

Li, Z., Chan, T., & Zheng, R. (2003). Statistical analysis of online strain response and its application in fatigue assessment of a long-span steel bridge. *Engineering structures, 25*, 1731-1741.

Li, Z., Wu, B., & Wang, Y. (2009). Statistical analyses on multi-scale features of monitoring data from health monitoring system in long cable supported bridges. *Procedia Engineering, 1*(1), 123-127.

Lin, S., Yang,J.,& Zhou,L. (2005). Damage identification of a benchmark building for structural health monitoring. *Smart Materials and Structures, 12*, 162-169.

Mattson, S., & Pandit, S. (2006). Statistical moments of autoregressive model residuals for damage localisation. *Mechanical Systems and Signal Processing, 20*(3), 627-645.

Medda, A., Chicken,E. & DeBrunner,V. (2007). SIGMA-SAMPLING WAVELET DENOISING FOR STRUCTURAL HEALTH MONITORING. 119-122.

Meo, M., Zumpano, G., Meng, X., Cosser, E., Roberts, G., & Dodson, A. (2006). Measurements of dynamic properties of a medium span suspension bridge by using the wavelet transforms. *Mechanical Systems and Signal Processing, 20*(5), 1112-1133.

National Transportation & Safety& Board. (2007). from http://www.dot.state.mn.us/i35wbridge/index.html

Oh, C., Sohn, H., & Bae, I. (2009). Statistical novelty detection within the Yeongjong suspension bridge under environmental and operational variations. *Smart Materials and Structures, 18*, 1-9.

Omenzetter, O., & Brownjohn J. . (2006). Application of time series analysis for bridge monitoring. *Smart Materials and Structures, 15*, 129-138.

Pai, P., Huang, l., Hu, J., & Langewisch, R. (2008). Time-frequency method for nonlinear system identification and damage detection. *Structural Health Monitoring, 7*(2), 103-125.

Peng, Z., Tse, P., & Chu, F. (2005). A comparison study of improved Hilbert-Huang transform and wavelet transform: Application to fault diagnosis for rolling bearing. *Mechanical Systems and Signal Processing, 19*(5), 974-988.

Pines, D., & Salvino, L. (2006). Structural health monitoring using empirical mode decomposition and the Hilbert phase. *Journal of sound and vibration, 294*(1-2), 97-124.

Polikar,R.(2001).TheWavelet Tutorial. from http://users.rowan.edu/~polikar/wavelets/wtpart1.html

Report Card for America's Infrastructure. (2005). *ASCE (American Society of Civil Engineers),* from http://www.asce.org/reportcard/2005/index.cfm.

Report Card for America's Infrastructure. (2009). *ASCE (American Society of Civil Engineers)*from http://www.asce.org/reportcard/2009/

Rohrmann, R., Baessler, M., Said, S., Schmid, W., & Ruecker, W. (1999). *Structural causes of temperature affected modal data of civil structures obtained by long time monitoring.* Paper presented at the Proceedings of the XVII International Modal Analysis Conference.

Shinde, A., & Hou, Z. (2004, June 30-July 2). *A wavelet packet based sifting process and its application for structural health monitoring.* Paper presented at the American Control Conference, Massachusetts.

Shumway, R., & Stoffer, D. (2000). *Time series analysis and its applications*: Springer Verlag.

Sohn, H., Allen, D., Worden, K., & Farrar, C. (2005). Structural damage classification using extreme value statistics. *Journal of dynamic systems, measurement, and control, 127,* 125-132.

Sohn, H., Czarnecki, J., & Farrar, C. (2000). Structural health monitoring using statistical process control. *Journal of Structural Engineering, 126*(11), 1356-1363.

Sohn, H., & Farrar, C. (2000a). *Statistical process control and projection techniques for damage detection*.

Sohn, H., & Farrar, C. (2000b). *Statistical Process Control And Projection Techniques For Structural Health Monitoring*.

Sohn, H., Farrar, C., Hunter, N., & Worden, K. (2001). Structural health monitoring using statistical pattern recognition techniques. *Journal of dynamic systems, measurement, and control, 123*, 706-711.

Sohn, H., Farrar,C.,Hemez,F.,Shunk,D.,Stinemates,D.& Nadler,R. (2003). A Review of Structural Health Monitoring Litreature:1996-200. *Los Alamos National Labratory Report*(LA-13976-MS).

Sohn, H., Fugate, M., & Farrar, C. (2000). *Continuous structural monitoring using statistical process control*.

Staszewski, W., Read, I., & Foote, P. (2000). *Damage detection in composite materials using optical fibers- recent advances in signal processing.* Paper presented at the Proceedings of SPIE.

Taha, M., Noureldin, A., Lucero, J., & Baca, T. (2006). Wavelet transform for structural health monitoring: a compendium of uses and features. *Structural Health Monitoring, 5*(3), 267-289.

Wang, Z., & Ong, K. (2008). Autoregressive coefficients based Hotelling's T2 control chart for structural health monitoring. *Computers & Structures, 86*(19-20), 1918-1935.

Wang, Z., & Ong, K. (2009). Structural damage detection using autoregressive-model-incorporating multivariate exponentially weighted moving average control chart. *Engineering structures, 31*(5), 1265-1275.

Wong, K. (2001). *The wind and structural health monitoring system (WASHMS) for cable-supported bridges in Tsing Ma control area.* Paper presented at the Proceedings of the IFAC Conference on New Technology for Computer Control, Hong Kong.

Xu, Y., & Chen, J. (2004). Structural damage detection using empirical mode decomposition: experimental investigation. *Journal of Engineering Mechanics, 130*, 1279.

Yan, G., Duan, Z., Ou, J., & De Stefano, A. (2010). Structural damage detection using residual forces based on wavelet transform. *Mechanical Systems and Signal Processing, 24*(1), 224-239.

Yang, J., Lei, Y., Lin, S., & Huang, N. (2004). Hilbert-Huang based approach for structural damage detection. *Journal of Engineering Mechanics, 130,* 85-95.

Zalt, A., Meganathan,V., Yehia,S., Abudayyeh,O., Abdel-Qader,I. (2007). *Evaluating Sensors for Bridge Health Monitoring.* Paper presented at the Electro/Information Technology, 2007 IEEE International Conference.

Zemmour, A. I. (2006). *The Hilbert Huang transform for damage detection in plate structures.* University of MarylandCollege Park.

Zhu, B., Leung, A., Wong, C., & Lu, W. (2008). On-line health monitoring and damage detection of structures based on the wavelet transform. *International Journal of Structural Stability and Dynamics, 8*(3), 367-387.

Zuo, D., & Jones, N. P. (2010). Interpretation of field observations of wind- and rain-wind-induced stay cable vibrations. *Journal of Wind Engineering and Industrial Aerodynamics, 98*(2), 73-87.

VITA

Ermias Belay Biru

Candidate for the Degree of

Master of Science

Thesis: STRUCTURAL HEALTH MONITORING FOR BRIDGES USING ADVANCED DATA ANALYSIS FOR PROCESS NON-LINEARITY AND NON-STATIONARITY

Major Field: Industrial Engineering and Management

Biographical:

Education:

Completed the requirements for the Master of Science in School of Industrial Engineering and Management at Oklahoma State University, Stillwater, Oklahoma in December, 2010.

Completed the requirements for the Bachelor of Science in Industrial Engineering at Bahir Dar University in July 2004.

Experience:
Worked in the positions of Auto CAD draftsman, Site supervisor and Office Engineer at Lead COM integrated solutions.(November 2004-November 2008).

Professional Memberships:
Alpha Pi Mu, National Industrial Engineering Honor Society
Member of the Ethiopian Society of Industrial Engineers (ESIE)

Name: Ermias Belay Biru Date of Degree: December, 2010

Institution: Oklahoma State University Location: Stillwater, Oklahoma

Title of Study: STRUCTURAL HEALTH MONITORING FOR BRIDGES USING ADVANCED DATA ANALYSIS FOR PROCESS NON-LINEARITY AND NON- STATIONARITY

Pages in Study: 99 Candidate for the Degree of Master of Science

Major Field: Industrial Engineering and Management

Scope and Method of Study: The proposed research is focused on data analysis using time series modeling approaches, frequency domain analysis and statistical hypothesis testing for the purpose of Structural Health Monitoring. In this study a detailed time series modeling for data obtained from a functional bridge is investigated. The relationship between measured deformation values from different sensors installed on a bridge column is studied. The study also showed the relationship between temperature and deformation measured by sensors installed on the column of the bridge. Spectral analysis approaches which include Fourier transform, wavelet analysis and Hilbert transform are applied for a bench mark problem using simulation data. A statistical hypothesis testing is also applied in conjunction with the Hilbert transform to differentiate between a change in mean and variance of instantaneous frequency of the simulated data which was obtained from normal and damaged conditions of a structure.

Findings and Conclusions: The research showed that the applied time series and spectral analysis methodologies are effective for SHM application. From the analysis of bridge sensor data it is shown that the deformation developed in the columns of a bridge was increasing through time and also there exists a high correlation between temperature and deformation recorded by the sensors. A case study was developed to show the effectiveness and validity of the frequency domain approaches. A change in frequency is observed from the Fourier analysis when data gathered from a damaged and undamaged state is considered. The wavelet approach was successful in capturing change of scale (frequency) with time. From the comparison of the spectral analysis presented the Hilbert transform and empirical mode decomposition (EMD) were found to be the best approach compared with Fourier and wavelet analysis since it showed change in frequency at any instant of time. Coupled with statistical hypothesis testing, the Hilbert transform detected the change in the mean and variance of instantaneous frequency through time which signifies the presence of damage.

ADVISER'S APPROVAL: Zhenyu (James) Kong